Cement and Concrete Research 165 (2023) 107071

Contents lists available at ScienceDirect

Cement and Concrete Research

journal homepage: www.elsevier.com/locate/cemconres

Phase changes in cementitious materials exposed to saline solutions

Klaartje De Weerdt [a], Ellina Bernard [b], Wolfgang Kunther [c], Malene Thostrup Pedersen [a], Barbara Lothenbach [a,b,*]

[a] NTNU, Department of Structural Engineering, 7491 Trondheim, Norway
[b] Empa Swiss Federal Laboratories for Materials Science and Technology, Laboratory Concrete and Asphalt, Überlandstrasse 129, 8600 Dübendorf, Switzerland
[c] DTU, Department of Environmental and Resource Engineering, Brovej, Building 118, 2800 Kgs. Lyngby, Denmark

ARTICLE INFO

Keywords:
Concrete
Leaching
Seawater
Sulfate
Carbonation

ABSTRACT

This article summarizes long-term degradation mechanisms of cementitious materials in contact with fresh and saline solutions based on a review of experimental observations in field and laboratory studies. In addition, a simplified thermodynamic modelling approach was used to calculate the effect of the solution composition, ranging from river water to sea water, on the intensity of leaching and the kind and quantity of phases formed at the interface with the environment. This study shows that leaching is the main underlying degradation mechanism for all investigated exposure solutions. The presence of carbonates and sulphates in the solution increases leaching and decalcification of Ca-rich phases leading to the precipitation of calcium carbonate and calcium sulfate, while the presence of chloride has little influence on the intensity of leaching. Carbonates in the interacting solution can suppress ettringite formation. If present, magnesium precipitates as brucite, M-S-H or hydrotalcite-like phase.

1. Introduction

Cementitious materials are commonly used for structures exposed to saline solutions requiring a long service life. Examples are concrete infrastructure such as bridges, tunnels and dams exposed to solutions ranging from fresh water, seawater, de-icing salts to even sulphate containing ground water. The design service life for concrete infrastructure is often 100 years or more. Another critical application of cementitious materials is nuclear waste storage facilities, where a service life of 300 years or more is required. The concrete used for long-term storage facilities is exposed to saline solutions in contact with the surrounding rock or clay. Longer service lives are also required for offshore oil wells, which are often injected with aqueous solutions based on seawater to increase the well productivity. At the end of the production life of these wells, cement plugs are used to close the well. The integrity of these plugs depends on the interaction between production water in the reservoir, or the seawater, which both contain chloride, sulphate and carbonate ions. In order to ensure the longest service life possible of these structures, there is a need to understand the long-term degradation mechanisms of cementitious materials in contact with saline solutions.

Studies of the interaction between cementitious materials and saline solutions often concentrate on either chloride ingress in reinforced concrete, sulphate attack for concrete exposed to ground water or leaching in connection to long-term storage facilities. A comprehensive state of the art report on performance of cement-based materials in aggressive aqueous environments was published in 2013 [1].

The aim of the current paper is to combine findings from long-term field studies, laboratory experiments and thermodynamic modelling in order to identify common degradation features for a variety of exposure solutions. We specifically focus on exposure under submerged conditions to fresh water, NaCl solutions, rock and clayey water, seawater and sulphate containing solutions, as most relevant for applications. The paper concentrates on the interaction between these multi-component solutions and Portland cement pastes, while the potential interaction with the aggregates is not considered. The focus is on the chemistry of the systems, more specifically on the phase changes caused by the exposure conditions based on the predicted phase compositions, the potential changes in porosity or softening of the cement paste. The impact of porosity, pore structure, interfacial transition zone, the water-to-binder ratio, or of the resulting mechanical properties of concrete that affect the longevity of concrete, are not the focal point of this work.

* Corresponding author at: Empa, Swiss Federal Laboratories for Materials Science and Technology, Laboratory Concrete and Asphalt, Überlandstrasse 129, 8600 Dübendorf, Switzerland
E-mail address: barbara.lothenbach@empa.ch (B. Lothenbach).

https://doi.org/10.1016/j.cemconres.2022.107071
Received 31 March 2022; Received in revised form 6 December 2022; Accepted 19 December 2022

In a first section, the compositions of the investigated solutions and Portland cements are presented. These are used as input for a simple thermodynamic model to predict the phase changes caused by exposure to these solutions. The modelled phase compositions are compared with experimental findings from long-term field exposed concrete as well as laboratory exposed samples for each of the investigated solutions.

The interaction between the cementitious materials and rock or clay are more complex compared to sea water exposure although we modelled identical exposure volumes for both cases. In reality, the exposure conditions in contact with rock or clay are not constant as they are influenced by the exchange rate of ground water.

The combined approach of modelling and experiments enabled us to identify that leaching is one of the main underlying degradation mechanism for concrete exposed to saline solutions independent of the variations in exposure conditions. The various ions and their concentrations present in the exposure solution will determine the amount and the type of solids observed to precipitate in the leached cement paste.

2. Composition of solutions

The surface of concrete will interact with the environment, either with the CO_2 and humidity present in the air, or if submerged, with the surrounding solution. The latter being the focus of the current paper. High concentrations of salts of several hundreds of mM are present in seawater (Table 1) as well as in solutions often used in laboratory experiments to study resistance against chloride or sulphate, while freshwater in rivers and lakes contains very low concentrations of various salts. The composition of river or lake waters as well as the compositions of solutions in contact with clay stones or granite depend strongly on the minerals present in the surrounding rocks and catchment area and can vary largely between different locations as illustrated in Table 1 and Fig. 1.

Freshwater present in rivers and lakes generally contains only low amounts of Ca, Na, K, Mg, Si, Al, sulphate, chloride and carbonate as exemplified by the composition of the water from a Swedish river given in Table 1 and described in Fig. 1. The concentrations of the various constituents of fresh water generally show only small variations and are in the range from 0.01 to 0.2 mM, with pH values in the range of 6.5 to 8.5 [2]. The largest variation is observed for carbonate concentrations

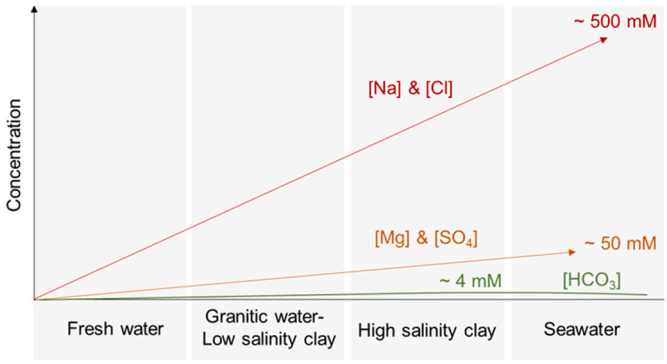

Fig. 1. Concentrations in the different solutions studied. All solutions exhibit a similar pH between 6.9 and 8.2. The chosen examples correspond to the case studies of degradation of cementitious materials in contact with saline solutions in Section 4.

(generally in the range 0.1 to 5 mM), which are influenced by the availability of $CaCO_3$ in the environment as well as from the decomposition of organic materials supplying additional CO_2.

The water present in granitic rocks has a more variable composition. Some of the granitic waters, such as the one from Grimsel in the Swiss Alps, have similar low elemental concentrations as the river water from Sweden reported in Table 1. Other granitic rock waters, such as the one from Äspö in Sweden, contain much higher NaCl concentrations in the range of 20 to 80 mM, similar to the pore waters of clayey rocks (COX and Tournemire claystone, see Table 1 & Fig. 1). The solutions present in clays can contain even higher salt concentrations, as exemplified by the solution in Opalinus claystone and bentonite (MX 80, see Table 1 & Fig. 1). These clay waters have chloride concentrations between 250 and 400 mM, i.e. concentrations similar to the chloride concentrations in seawater (Table 1 & Fig. 1). The salinity of a claystone depends on its time of formation and on the equilibrium of the aquifers [3]. The clay waters have neutral or slightly basic pH values and contain relatively high Na, Ca, Mg, carbonate and sulphate concentrations, which will influence their interaction with cements.

The temperature, composition and salinity of seawater differs

Table 1
Composition of the various exposure solutions discussed in this paper comprising river water, pore water solutions of different host rocks, sea water, and laboratory produced solutions such as NaCl, sulphate and bicarbonate mixture solutions (in mM). In addition, a typical pore solution composition for hydrated Portland cement paste is provided. The compositions of the solutions used for thermodynamic modelling are marked with [f], while the other values are given for comparison.

Solutions	K	Na	Ca	Mg	Al	Si	SO_4	Cl	HCO_3	pH	Ref.
	mM									–	.
River water (Ångermanälven)[f]	0.01	0.052	0.098	0.033	0.001	0.048	0.032	0.17[d]	0.11[e]	6.9	[16]
Granitic water (Grimsel)	0.004	0.67	0.14	<0.0001	0.001	0.24	0.06	0.15	0.5[e]	9.5	[17]
Granitic water (Äspö)[f]	0.2	56.6	8.88	3.22	n.d.	0.26	2.42	75.6	0.5[e]	8.2	[18]
Tournemire claystone[a]	0.8	23.5	1.5	0.7	n.d.	0.03	9.5	4.5	4.6	7.4	[19]
Callovo-Oxfordian (COx) claystone [b]	1	45.6	7.4	6.7	n.d.	0.2	15.6	41	3.3	7.1	[20]
Opalinus claystone [cf]	1.4	236.8	15	15.9	n.d.	n.d.	13.7	266.6	2.3[e]	7.6	[21]
Febex bentonite	2.6	330	68	81	n.d.	0.18	19	420	0.5[e]	7.4	[22]
Sea water (Baltic)	1.8	93	1.2	10.7	n.d.	n.d.	17.8	110	n.d.	n.d.	[23]
Sea water (Trondheim Fjord)	8.9	411	8.8	47	n.d.	n.d.	26.9	548	n.d.	n.d.	[24]
Sea water (Atlantic ocean)	9.7	457	10	56	n.d.	n.d.	27.8	536	2.3	n.d.	[25]
Standard sea water[f]	10.6	485	10.5	55	n.d.	n.d.	29.3	566	1.9	7.7.	[26]
NaCl solution (3 %)[f]	n.d.	545	n.d.	n.d.	n.d.	n.d.	n.d.	545	n.d.	7.1	[24]
Sulphate solution[f]	88	264	88	88	n.d.	n.d.	352	n.d.	n.d.	7.1	[27]
Bicarbonate solution[f]	88	614	88	88	n.d.	n.d.	352	n.d.	350	7.6	[28]
Pore solution of Portland paste	532	279	1.2	n.d.	0.31	0.29	27.6	n.d.	n.d.	13.7	[29]

n.d. = not determined.
[a] Tournemire argillite, IRSN's in-situ laboratory.
[b] COx argillite: Bure, France, Cigéo project, ANDRA.
[c] Opalinus clay: St-Ursanne, Switzerland, Mont-Terri project, NAGRA.
[d] Adapted for electroneutrality.
[e] Equilibrated with calcite.
[f] Solution used for thermodynamic modelling.

between oceans and the salt concentration of the seawater can vary from location to location and time of year, for example due to dilution by fresh water from rivers. However, the proportions of the constituents are essentially constant and on average, seawater contains a total of about 35 g/L dissolved salts as shown in Table 1. The composition of seawater in the Trondheim Fjord, the Atlantic Sea, and the standard sea water composition are comparable, while water from the Baltic Sea has somewhat lower concentrations due to a higher dilution. It might thus be expected that the combined chemical impact of the different ions present in seawater is comparable for marine-exposed structures [4,5]. Seawater has a pH within the range of 7.8 to 8.3.

The pore solution present in freshly hydrated Portland cement exhibits pH values in the range of 13 to 13.7, due to the high alkali content of the cement [6,7]. These pore solutions are also characterized by high Na and K concentrations, which often reach a few hundred mM (Table 1) as well as by calcium and sulphate concentrations in the mM range, while the concentrations of other elements such as silica, aluminium and magnesium are generally lower. Calcium and alkalis have been observed to leach out of the cement paste. In the case of interaction with sea or fresh water this can, in the short-term, be expected to lead to an increase of pH and alkali concentration near the surface of the concretes structure, while in the long-term the effect will be negligible, as rivers, lakes and the sea represent, in comparison with a concrete structure, a nearly endless reservoir. Hydroxide, calcium and alkali ions will also migrate into clays, clay rocks and granite to compensate for pH and concentration differences. Due to the limited amount of solution in such rocks, the high pH values and alkali concentrations present in fresh cement paste can increase the pH of the surrounding solution as well. The alkali and calcium ions will diffuse into the environment as a hyperalkaline plume. This high pH can lead to the partial dissolution of clayey-rocks [8,9], clays [10,11] and accessory minerals such as calcite, dolomite, and quartz [12,13]. In addition, the high calcium concentration from cement pore solution can exchange with the cations adsorbed on clays releasing Na and Mg [14,15]. However, also the pore solution of the cement near its surface will be modified by the increased Mg, Si and Al concentrations released in the pore solutions of the clays and clay rocks due to the dissolution of solids.

3. Thermodynamic modelling

The composition of hydrated cements and the changes upon the interaction with different solutions can be calculated by thermodynamic modelling as demonstrated for many applications [24,27,30,31] and illustrated in Fig. 2. Thermodynamic modelling is carried out using the geochemical modelling code Gibbs Energy Minimization Selektor (GEMS) [32], which computes equilibrium phase assemblages and speciation in complex geochemical systems. The general thermodynamic data were selected from the PSI/Nagra thermodynamic database [33], complemented with solubility products for cement hydrates [34], zeolitic phases [35–37] and layered-double hydroxides (hydrotalcite-like LDH) with different anions in the interlayer [38]. The composition of calcium silicate hydrates (C-S-H) was modelled using the "CSHQ" model [39], which accounts for the uptake of alkali in the C-S-H phase [34]. The formation of quartz (SiO_2), dolomite ($CaMg(CO_3)_2$), aluminium containing siliceous hydrogarnet ($((CaO)_3(Al,Fe)_2O_3(SiO_2)_{0.84}(H_2O)_{4.32}$), goethite (FeOOH), hematite (Fe_2O_3) and of some zeolitic phases (natrolite, heulandite and stilbite) was suppressed in the calculations due to kinetic reasons, while the solubility of brucite was increased by 0.5 log units.

The composition of the cements used to calculate the hydrate assemblage is detailed in Table 2. Two different Portland cement compositions were considered. In general, a Portland cement composition corresponding to the Portland cement (PC1) used in the experiments of De Weerdt et al. [24] for samples exposed to seawater and NaCl solution was used. For the cement exposed to clay solution (PC2), the composition of the cement actually used in those experiments [40] was considered to allow direct comparison with the transport modelling presented in [12]. The composition of the hydrated cements (without interaction with the environment) is shown on the right-hand side of each graph in Fig. 2. A hydrate assemblage consisting of C-S-H, ettringite, portlandite, monocarbonate, iron-containing siliceous hydrogarnet, and hydrotalcite was calculated for both PC1 and PC2. Somewhat more hydrotalcite was predicted in the case of the magnesium rich PC2 (Fig. 2d), and unreacted calcite was predicted for PC1 only (Fig. 2a-c, e-g). The quantities of the other hydrates were very similar between the two cements.

Moving from right to left [30,31], the gradual changes towards the surface of the concretes exposed to the different solutions are displayed. The vicinity of the concretes to each solution is simulated by increasing the amount of exposure solution. This allows to mimic the changes observed experimentally towards the surface of cement, mortar or concrete specimens as detailed e.g. in [30,31]. Such simplified thermodynamic models are very flexible and allow easy parameter variations and the results are in many cases comparable to full transport modelling, where parameters such as porosity, tortuosity, ion specific diffusion coefficients and reaction kinetics have to be known in detail. For example, [31] neglected transport of ions in the simplified approach, which can lead to specific artefacts. A detailed comparison between the simplified modelling as used here and full transport modelling is given in [31] as well as in Section 4.4 in the present paper.

The composition of river, granitic, clay and sea water, and of the different solutions used in laboratory test (NaCl, sulphate and bicarbonate solution), as detailed in Table 1, were used in the models. A comparison of the different graphs shows that in fresh water, NaCl solution and granitic water leaching dominates, leading to the decalcification of C-S-H, the destabilisation of monocarbonate and/or Friedel's salt to strätlingite or zeolitic phases (Cl-sodalite) and a decrease of the solid volume near the surface (left hand side of the graphs). The term "leaching" is used in this paper to describe any removal of elements from a solid. The changes at the cement surfaces in contact with clay water and particular of that in contact with sea water are further influenced by the presence of sulphate, magnesium and carbonate, which lead to the formation of additional ettringite, as well as magnesium silicate hydrate (M-S-H) and calcite at the outer surface. For the chloride containing solutions (NaCl solution, seawater and to a lower extent also in the clay solution) in addition the destabilisation of monocarbonate in favour of Friedel's salt is predicted.

The presence of chloride is also mirrored in the anion occupancy of the AFm phases plotted at the bottom of each graph. Al_2O_3-Fe_2O_3-mono (AFm) phases are present as hydration products in PC. AFm phases have a layered double hydroxide (LDH) type structure, where Ca^{2+} in the main portlandite-like layer is partially replaced by Al^{3+} or Fe^{3+} resulting in a positively charged main layer. This charge is balanced by an interlayer containing various anions and H_2O. In PC without limestone, SO_4^{2-} would be the main anion resulting in the formation of monosulphate (C_4AsH_{12-16}), while in modern cements, where calcite is present, rather CO_3^{2-} is present and monocarbonate (C_4AcH_{11}) is here the main AFm phase [29,42]. In the presence of high chloride concentrations, the formation of Friedel's salt ($C_4ACl_2H_{10}$) can be expected [24,30], while Ca leaching is expected to stabilize strätlingite ($C_4A_2S_2H_{14-16}$) [43], which contains $Al(OH)_4^-$ and $SiO(OH)_3^-$ in its interlayer. In fact, the thermodynamic modelling in Fig. 2a-g confirms that carbonate is the dominant anion in AFm phases in the hydrated cements due to the presence of calcium carbonate. Nearer to the surface, interaction with the surrounding solutions leads to replacement of carbonate in AFm by chloride in the case of the NaCl solution, seawater and clay solution or by Al-Si-hydroxide in river water where strätlingite has formed. Neither sulphate nor hydroxide is calculated to be present in any significant amount in the interlayer of AFm phases, due to the high stability of monocarbonate compared to the other AFm phases [34].

In contrast, a mixed occupancy of carbonate and hydroxide is calculated to be present in the interlayer of hydrotalcite-like phases,

which have a weaker preference for carbonate [38] than the AFm phases. Hydrotalcite-like phases are Mg and Al based layered double hydroxide solids (Mg-Al-LDH, which will be referred to as LDH in the paper) with an isomorphic substitution of Mg^{2+} by Al^{3+} in the brucite-like main sheet, which generates positive charges. The main layer can have a variable Mg/Al ratio [44,45] and Al can be replaced by iron [46,47]. The positive charge in LDH is balanced by the presence of different anions, mainly hydroxide and carbonates in a hydrated Portland cement paste [44]. The uptake of a significant amount of chloride was not predicted to occur in LDH due to the relatively low stability of

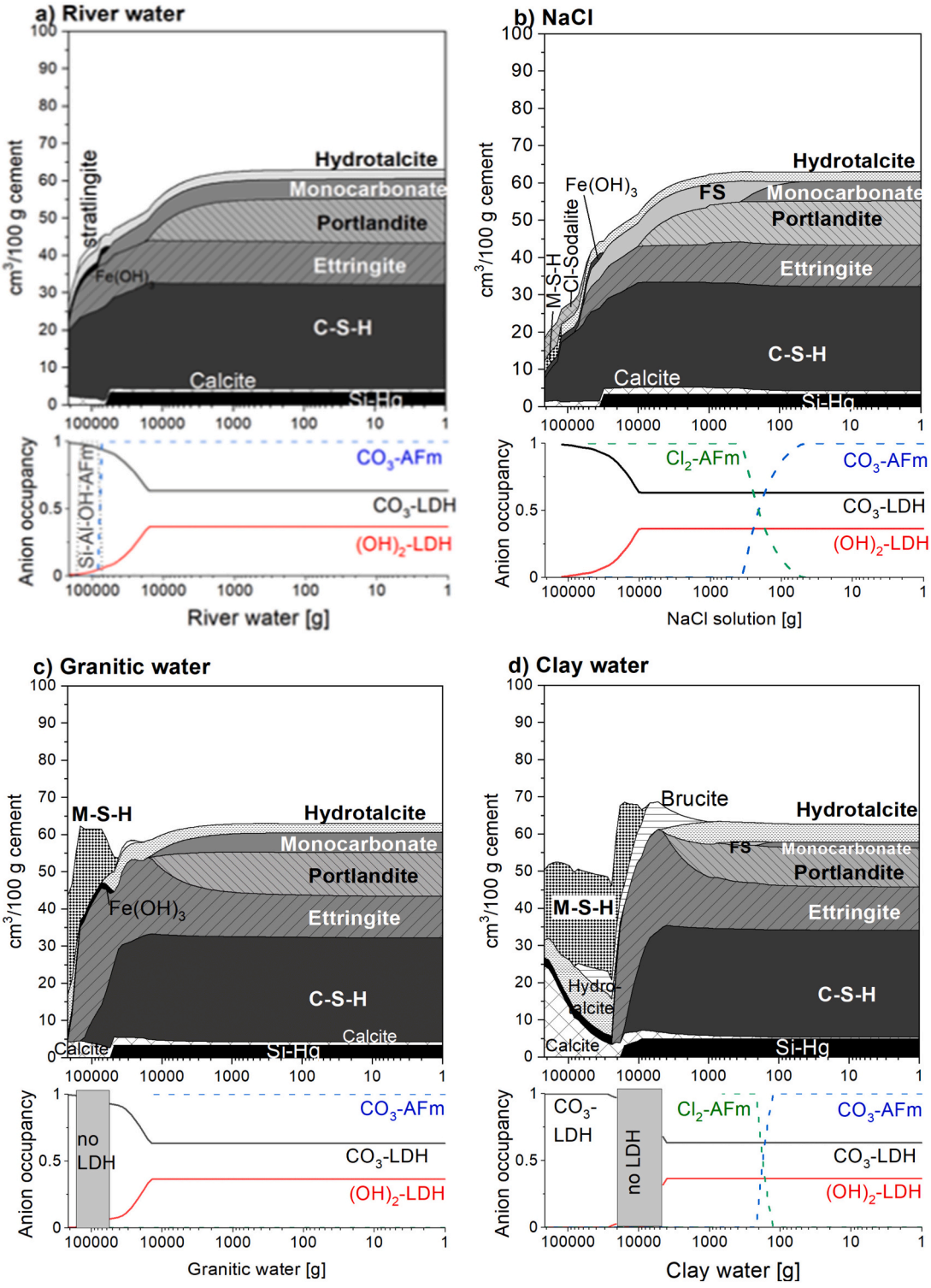

Fig. 2. Predicted volume of phases and anion occupancy in AFm and LDH phases in Portland cement paste (w/c = 0.4) exposed to increasing amounts of solutions (a) river water, (b) NaCl, (c) granitic water, (d) clay water, (e) sea water, (f) sulphate solution, and (g) bicarbonate solution. Solution composition detailed in Table 1. The phases are given in [cm^3/100 g cement] based on the PC1 composition from [24]; for the calculations with clay water PC2 [48] was used. AFm: Al-Fe-monophases, such as monocarbonate, monosulphate, strätlingite or Friedel's salt; C-S-H: calcium silicate hydrate, FS: Friedel's salt; LDH: layered double hydroxide, hydrotalcite-like phase; M-S-H: magnesium silicate hydrate; Si-HG: siliceous hydrogarnet.

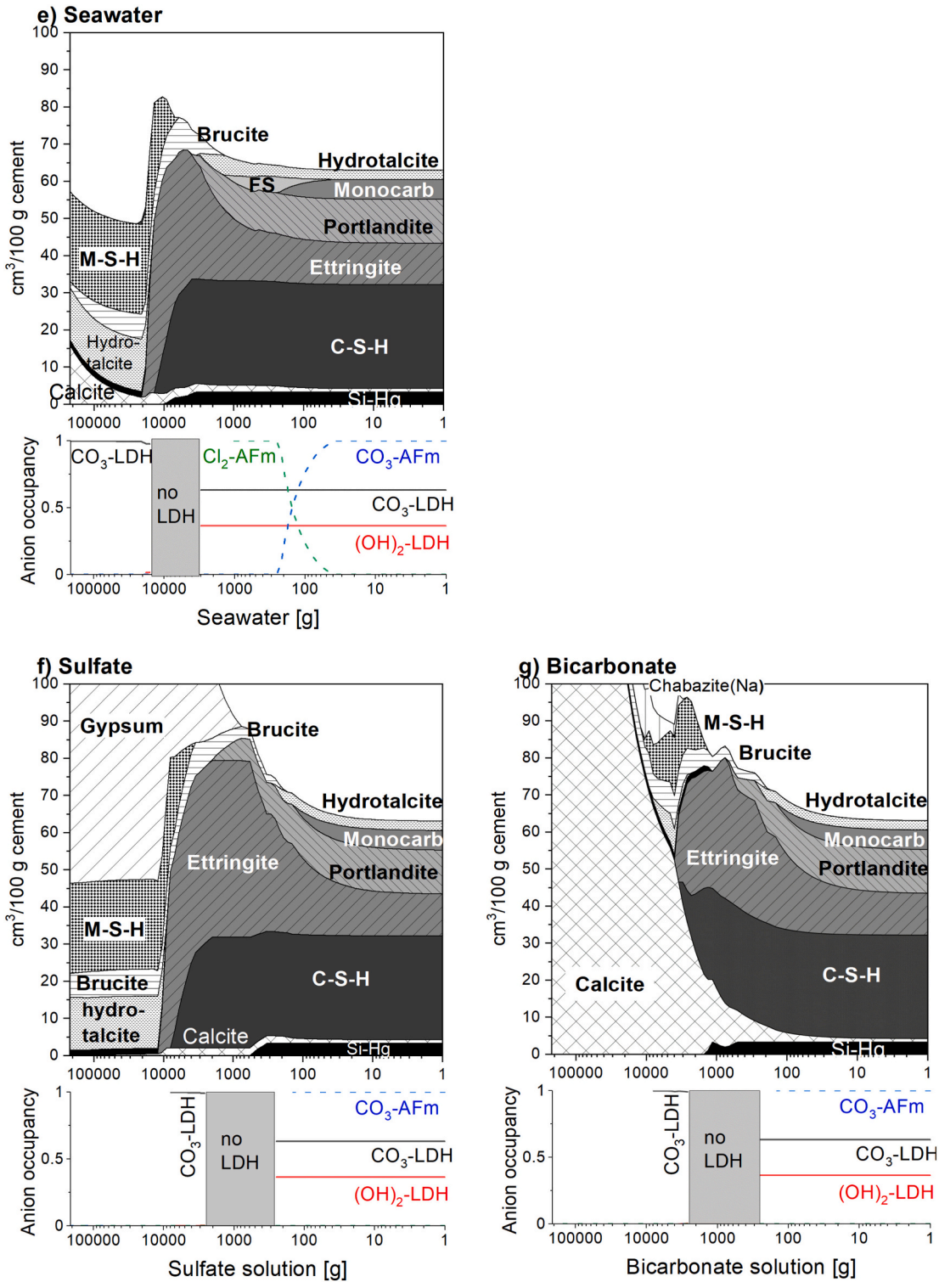

Fig. 2. (*continued*).

Table 2
Oxide composition of the two Portland cements (PC1 and PC2) used for the thermodynamic modelling (in wt%) determined by XRF. Water to cement ratio = 0.4.

	SiO_2	Al_2O_3	Fe_2O_3	CaO	MgO	K_2O	Na_2O	SO_3	CO_2	Ref.
PC1	19.6	4.5	3.5	61.6	2.4	1	0.5	3.4	1	[16,24]
PC2	20.6	3.9	5.2	58.8	4.6	0.75	0.27	3.5	1.4	[41]

Cl-LDH [38].

Independent of these differences, leaching of Ca-rich phases is the main degradation mechanism calculated, as visible in the destabilisation of portlandite, of AFm phases such as monocarbonate and of C-S-H towards to surface of the specimen. This leaching is also accompanied by the destabilisation of ettringite, siliceous hydrogarnet, and finally LDH (hydrotalcite) at the leached surface. Strätlingite or zeolitic phases, such as Cl-sodalite or chabazite, M-S-H and $Fe(OH)_3$ are predicted to form instead at the surface in all cases (note that calcite and M-S-H formation in the case of river water is calculated at higher amounts of solution than displayed in Fig. 2).

A decrease of the calculated pH from 13.7 in the hydrated cement to a pH below 12 in the case of river and granitic water and NaCl solution and to below pH 10 for the carbonate and sulphate-rich solutions (seawater, clay water, sulphate and bicarbonate solution) is calculated by thermodynamic modelling. Fig. 2 shows also that the presence of carbonate and sulphate in the interacting solutions leads to an increased degradation of calcium rich phases such as portlandite due to formation of calcite and gypsum, which bind calcium originating from the PC. The presence of magnesium in the interacting solutions leads to the formation of M-S-H and/or brucite at pH values above 10.5, as well as of additional hydrotalcite if sufficient aluminium is present.

4. Case studies of degradation of cementitious materials in contact with saline solutions

4.1. Fresh water

The long-term changes in a concrete in a 55-year-old dam in the North of Sweden exposed to river water (composition listed in Table 1) was investigated by Rosenqvist et al. [16]. Using cores drilled at and below the water level (−10 and − 18 m), they identified experimentally 5 different zones in the leached concrete, see Fig. 3. Zone 1 represents the unaltered zone which is rich in calcium, corresponding to the presence of calcium rich hydrates such as portlandite, Ca-rich C-S-H and ettringite expected in Portland cement as illustrated on the right-hand side of Fig. 2a. In the submerged concrete, portlandite and ettringite appeared to have redistributed in zone 1 and filled air voids, which was not observed in the concrete above the water level.

In zone 2, they observed calcium leaching. They attributed this primarily to dissolution of portlandite, though the dissolution of portlandite alone could not explain the drop in CaO. Thus, C-S-H might already start to decalcify and AFm phases such as monocarbonate might also start to decompose to stratlingite in this zone. This is in agreement with the thermodynamic calculations in Fig. 2a, which illustrate that first portlandite is expected to dissolve, followed by the decomposition of AFm and decalcification of C-S-H.

Note that in zone 2, a moderate enrichment in sulphur is observed, which could be related to the formation of secondary (non-expansive) ettringite from sulphur and aluminate originating from decomposed AFm and AFt from more outer-laying zones, e.g. zone 5 in Fig. 3, which seems to be depleted for sulphur. Similar observations were made by Faucon et al. [49,50] for water exposed cement paste. This effect is not captured by the simple thermodynamic model in Fig. 2, which does not account for the movement of ions inwards into the cement paste, as discussed in more detail in [31], but considers merely the increase in the amount of exposure solution in contact with the cement paste.

In zone 4, a considerable change in the cement paste composition has been observed. The CaO content decreases even further, whereas the relative MgO content increases, thereby implying further decalcification of the C-S-H as well as a loss of mass. In zone 5, the magnesium content increases even further, and nodules of M-S-H are observed as well as the presence of calcium carbonate, explaining the peaks in CaO in this zone. Both C-S-H and M-S-H are nano-crystalline [46]. C(-A)-S-H phases have a CaO main layer with Si chains on both sides while M-S-H consists of brucite type main layers intermixed with silicate layers in T-O and T-O-T arrangement similar to clay minerals [51,52]. The carbonates and magnesium originate from the river water, and their formation is also predicted by the thermodynamic model (although not displayed, as M-S-H and calcite formation are predicted at very high solution concentrations, outside the range shown in Fig. 2). This could be an artefact of the simplified modelling approach used here, where the transport of Ca$(OH)_2$ away from the cement into the environment is neglected.

Rosenqvist et al. [16] describe zone 5 as a kind of dense crust on the concrete while zone 4 is a weak and porous zone, making it easy to mechanically remove the crust. The crust was not observed in the concrete core extracted at the water level, as the concrete at this level was exposed to frost scaling and abrasion by ice, removing this outer crust and exposing coarse aggregates and a new cement paste surface. No strong variation in sodium and potassium content in the concrete core was reported.

4.2. NaCl solution

De Weerdt et al. [24] investigated the phase changes in mortar exposed to a 3 % NaCl solution. The phase changes predicted by thermodynamic modelling are similar to those of the river water as shown in Fig. 2a and b: leaching at the surface including destabilisation of portlandite, ettringite, AFm, and LDH phases, while M-S-H and $Fe(OH)_3$ are calculated to form. In contrast to the river water, no additional calcite is calculated to form due to the absence of bicarbonate in the interacting solution, but the formation of Friedel's salt and of chloride-sodalite, a

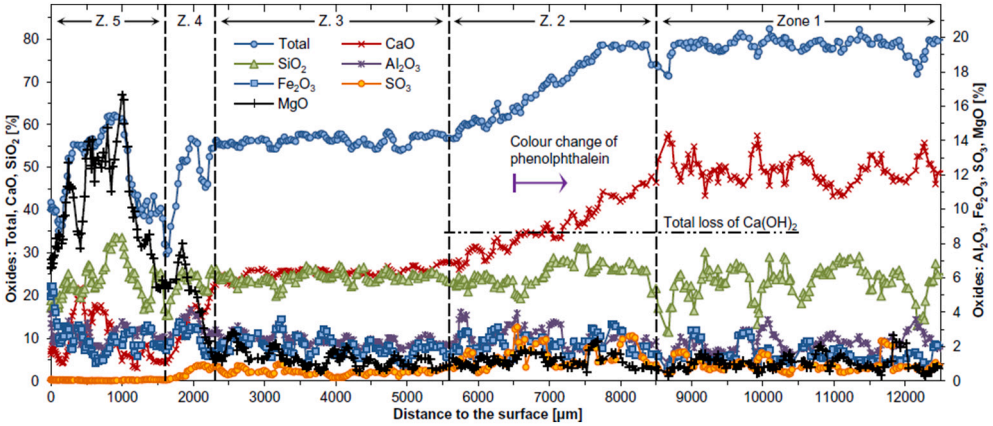

Fig. 3. Alteration observed in the chemical composition of a concrete exposed for 55 years to river water determined by electron microprobe analysis normalised to 100 %, reproduced from Rosenqvist et al. [16].

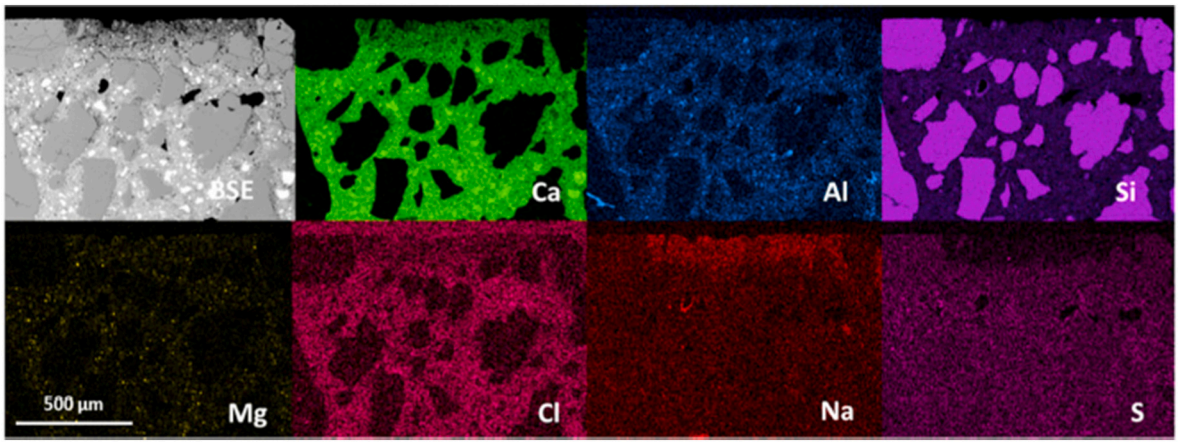

Fig. 4. Elemental maps of the surface of a PC mortar exposed for 90 days to a 3 % NaCl solution, reproduced from De Weerdt et al. [24].

chloride containing zeolitic phase are predicted. A similar thermodynamic model predicting leaching and the formation of Friedel's salt has been first presented by Looser et al. [30]. The back scatter electron image of the mortar samples exposed for 90 days to the NaCl solution [24] in Fig. 4 show in fact a significant leaching at the exposed surface at the top end of the maps.

The elemental map of calcium in Fig. 4 illustrates the strong leaching of calcium during exposure to NaCl solution, similar to the observation of Rosenqvist et al. [16] in Fig. 3 for exposure to river water. The intensity of the calcium map is considerably reduced in the outermost 100 µm, indicating a destabilisation of portlandite, ettringite and decalcification of C-S-H. In fact, a clear decrease in the portlandite content was measured using thermogravimetric analysis in the first 1 mm near the surface. Fig. 4 illustrates also that no precipitation of calcium carbonate occurs at the surface of the mortar, in agreement with modelling calculations presented in Fig. 2b.

In the outermost calcium leached zone (100 µm), very low sulphur intensities are observed in the sulphur map in Fig. 4, indicating that the sulphate containing hydrates such as ettringite are destabilized in this zone. However, further inside higher sulphur intensities are present, with no clear zoning although a slight indication of an enrichment at about 250 µm depth is visible (see Fig. 4).

Chloride intensities are also low in this intense calcium leached zone (outermost 100 µm), see Fig. 4, while after this zone the chloride levels in the cement paste rise rapidly. The relatively high chloride content in the cement paste can be attributed to chemical binding of chlorides in the AFm which is also predicted by the model as Friedel's salt (FS) and chloride-sodalite in Fig. 2b). In addition, chlorides can physically be bound in the C(-A)-S-H [5,53–61], although the thermodynamic model does not account for this yet. The physical binding can stand for a large part of the chloride uptake in hydrated cement paste [60,62].

In contrast to chloride, Na is enriched only in the outermost 100 µm of the cement paste, i.e. in the calcium depleted zone. This might be attributed to an increased Na uptake in the low Ca/Si C-S-H present near the surface, as the presence of less calcium strongly increases the sodium uptake in C-S-H [63–67]. In addition, a N-A-S-H phase (Na-containing zeolites) such as sodalite could have formed in the most leached zone of the cement paste, see Fig. 2b. Note, that if the formation of Cl-sodalite is not considered (as done in [24]), the formation of natrolite is predicted. In this context it is interesting to mention that an increase of KOH in NaCl exposure solutions limited strongly the observed leaching of portlandite, and also slowed down chloride ingress [68].

The experimental and the modelling data indicate that the major changes caused by the presence of NaCl solution are similar as to those in river water, a strong calcium leaching destabilising cement hydrates near the surface. The only considerable difference is the formation of chloride containing AFm, i.e. Friedel's salt, instead of monocarbonate, and the potential formation of chloride sodalite.

4.3. Granitic and low salinity clay water

Experimental studies of the changes at the interface between granitic rocks and cementitious materials are rare [69–71], while many detailed studies on the changes at the interface of cementitious materials with clays are available due to its importance for the long-term safety of geological repositories. Laboratory and in-situ experiments have provided detailed information on the mineralogical changes in the cement paste as well as in the adjacent claystone or bentonite [12,40,48,72–81]. As the solutions of some clayey rocks (e.g. COx and Tournemire clay) have similar elemental concentrations as some of the solutions in granites, their effect is discussed together in this section.

The few available experimental studies on changes at the cement granite interface were carried out in Grimsel after an interaction time of 4 to 13 years for a low salinity solution [70,71,82], (Table 1). Detailed characterization of both the cement and granite near the interface indicated no significant alteration of the granite, which might be related to relative short duration of the experiments. However, the outermost layer of the concrete was leached and its porosity increased; portlandite was absent, while ettringite, C-S-H, hydrogarnet and hydrotalcite were still observed [69]. EDX mappings indicated an increase of Mg near the surface as well as the formation of some calcium carbonate [71], which is in agreement with trends of the simple calculations in Fig. 2c, although the concentrations in Grimsel water are significantly lower (see the Grimsel water in Table 1) than in the Aspö granitic water in Finland, which was used in the thermodynamic model. As in the case of river water, modelling indicates that the predominating effect of granitic water is the destabilisation of the Ca-rich phases, particularly of portlandite and monocarbonate and the decalcification of C-S-H near the surface. The formation of a limited amount of additional ettringite is modelled due to the presence of some sulphate (0.1–2 mM, Table 1) in granitic waters, once portlandite and monocarbonate are destabilized. Ettringite and C-S-H are destabilized near the surface, while some M-S-H and a low quantity of calcite are calculated to form (Fig. 2). The degradation of concrete by COx solution is expected to be comparable based on the calculations presented in [83], leaching, decalcification of C-S-H and hydrotalcite precipitation (the potential formation of M-S-H was not considered, due to absence of thermodynamic data for M-S-H at that time).

Detailed studies are available for the COx clay - cement interface. The decalcification of Ca-rich phases has been observed experimentally in contact with COx water [84]. Interestingly, the formation of additional ettringite as well as some M-S-H near the interface was observed in [84] during the first months of interaction (see Fig. 5). The formation of a calcite-crust is the main degradation product observed

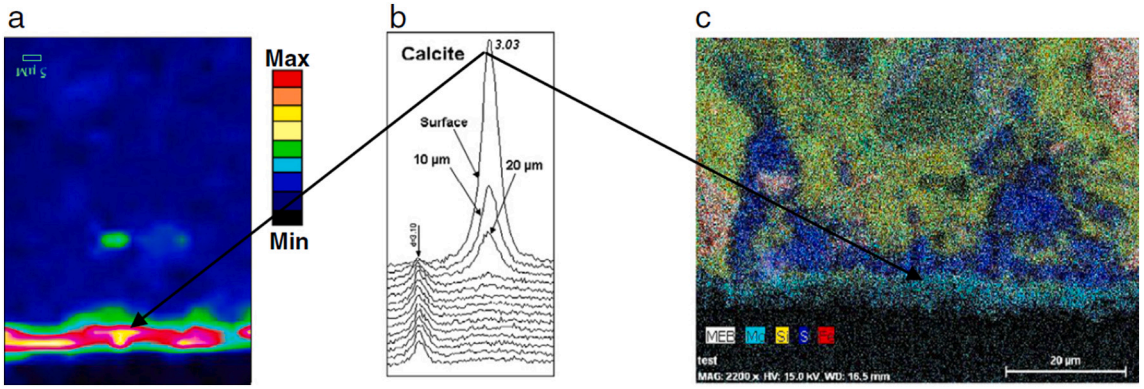

Fig. 5. a) Raman map, b) XRD and c) SEM-EDS mapping of a Portland cement paste exposed for 5 months to COx water; reproduced from [84].

experimentally for Portland cement paste in contact of COx, which contains more carbonates than the granitic water (Table 1). The formation of calcite at the interface reduces the porosity as well as the exchange of soluble species; this crust also contains magnesium, although the Mg concentration in COx is rather low with ~7 mM [84]. This is in agreement with the modelling presented in Fig. 2c.

At increased temperatures (50–80 °C), the formation of semi-crystalline C-A-S-H phases and zeolites was observed at the interface of cement with Tournemire clayey rock [85]; zeolite formation was also observed in batch experiments of cement hydrates with albite (representing a granite-like type rocks) [86].

4.4. High salinity clay waters

The simple thermodynamic model for Portland cements (using PC2) exposed to an increasing amount of pore water present in Opalinus clay (OPA, see Table 1) is presented in Fig. 2d. It shows, similar to granitic and river water, calcium leaching as visible in the destabilisation of portlandite and monocarbonate and a decalcification of C-S-H. In addition to the precipitation of M-S-H and calcite, the model predicts the precipitation of CO_3-hydrotalcite due to the relatively high Mg and carbonate concentrations in the clay water.

The destabilisation of the Ca-rich phases in the cement in contact with clay water has been confirmed experimentally [12,40,48,72–79]. Only one third of the initial calcium content in the Portland cement paste was still present in the first 1 mm after 10 years of interaction with OPA (Fig. 6). The experimental data indicate the migration of calcium from the cement across the interface into the OPA clay, which is the equivalent to the leaching in direct contact with waters. In the OPA clay, the calcium is taken up by the cation exchange sites of the clays, which then release magnesium and sodium to the OPA pore water, which diffuse into the cement as well as further into the clay ([75], see also Fig. 6b). The clayey pore solution migrates into the cement lowering the pH and destabilising the Ca-hydrates (portlandite, ettringite and C-S-H), resulting in complete depletion of portlandite and ettringite at the near surface and low Ca/Si C-S-H [74].

Calcite is usually formed at the interface with bentonite or OPA-clay, from the decalcification of portlandite and C-S-H and from the in-diffusion of bicarbonate from external pore water (atmospheric or at equilibrium with the clays pore solution) (see e.g. [48,72,73]). However, in some cases no crystalline $CaCO_3$ phases are observed [74], which could be due to the precipitation of amorphous calcium carbonates or to the high porosity of the concrete, thus strong leaching of Ca as detailed below.

Several SEM EDS studies at the interface with bentonite ([80,81,87], Fig. 6a) confirmed the precipitation of C-(A-)S-H with low Ca/Si and a relatively high Al/Si near the concrete surface after >4 years of interaction. This was due to the presence of Al in clay water near the interface where the high pH values imposed by the cement lead to a limited dissolution of the clay minerals. The presence of low Ca/Si C-S-H is also mirrored in the increased Na and K binding observed near the interface, as the lower amount of Ca in C-S-H leads to an increase in the alkali uptake [63–67].

For cement clay interaction, not only experimental studies but also reactive transport modelling are available for the long-term prediction of these types of interfaces (see e.g. [12,88–90]). The models account for variations in porosities but do often not include the latest thermodynamic data and/or are using simplified phase compositions. Fig. 7 shows the results of such a transport model illustrating the phase changes at the interface between Opalinus Clay in contact with Portland cement paste (i.e. the PC 2 used in Fig. 2d). The reactive transport model accounts for the transport of ions between the cement paste and clay and shows the destabilisation of the C-S-H and portlandite, in good agreement with the simplified model shown in Fig. 2d. At the interface and in the clay, the formation of hydrotalcite, brucite and calcite is predicted. The transport model predicts a different spatial distribution of the phases formed compared to the simplified model shown in Fig. 2d. This particular reactive transport model indicates a wide carbonation zone with a low calcite content as observed in [74] due to a high w/c (0.6) in the concrete instead of a layer of calcite at the interface predicted by the simplified model. The decrease in porosity due to the calcite formation limits the migration/leaching of the species and thus the deterioration kinetics. Whether the precipitation of calcite jointly with a decrease in porosity can lead to clogging at the interface is under debate [88–90].

A magnesium-enriched zone is also observed for cements in contact with clayey rock, but it can be detached from the interface, i.e. a few mm away, in the clay (see Fig. 6b) and d) and e.g. [75] [80]). In bentonites, the Mg enrichment is attributed to the neoformation of additional tri-octahedral phyllosilicates [91–93], namely M-S-H [51,52,94] as displayed in the simplified model in Fig. 2d. At the PC-OPA clay interface, there is no clear evidence of M-S-H precipitation as the OPA solution contains less Mg, and the formation of crystalline Mg phases such as brucite is not observed [74]. However, the observed magnesium enrichment is 4 times the possible amount of an entirely magnesium-exchanged clay [75] which indicates the formation of a new solid phase. The lower concentration of Mg in the clayey rock porewater (Mg in COx or OPA about 0.5–20 mM) compared to the Febex bentonite (70 mM) results in a lower Mg enrichment and higher uncertainties about the nature of the Mg-phases and is either due to i) the formation of nano-crystalline M-S-H or ii) the formation of poorly crystalline hydrotalcite as modelled in the Fig. 2d without transport. Additionally, the reactive transport (Fig. 7) could actually predict very well the precipitation of brucite and hydrotalcite in the clay side (as proxy for the Mg-phases).

The content of sodium (from NaCl) is higher in the Portland cement paste at the interface than in the unexposed paste. An increase of Al and Si is also observed at the interface (Fig. 6a and c). This could be due to additional precipitation of a phase containing Al, Si and alkalis such as C-A-S-H containing alkalis (as in bentonite) and/or typical zeolitic

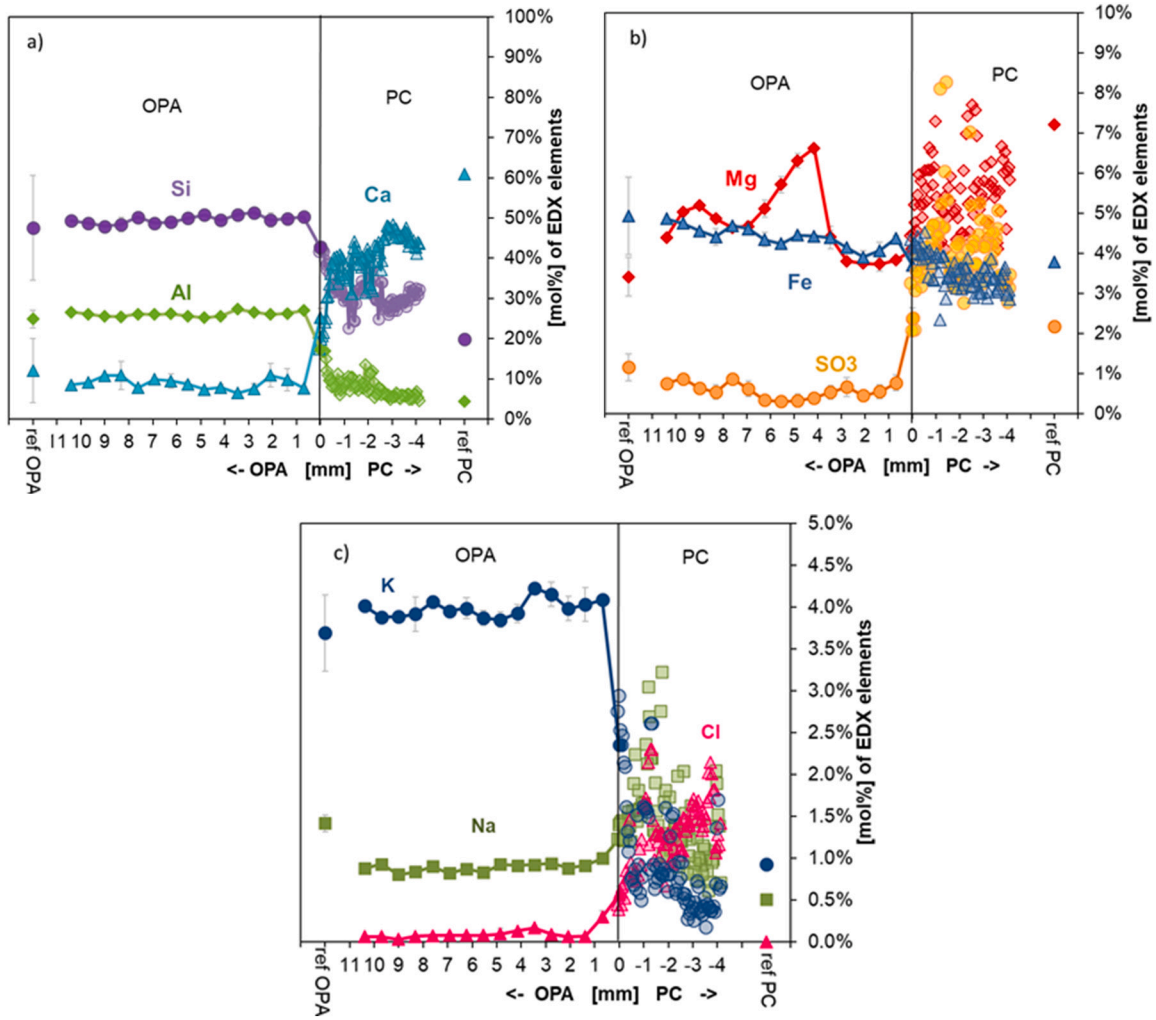

Fig. 6. a), b) & c) Elemental concentration profiles determined by EDS across the interface of Portland concrete in contact with OPA after 10 years. Dark symbols show the average composition of an area (including aggregate and sand) while the light symbols correspond to surface spot measurements chosen by hand in the homogeneous hydrated cement matrix close to the interface; adapted from [40]. Samples from the CI experiments from Mont-Terri (Switzerland).

precursors such as N-A-S-H gels. Increased temperature promotes the formation of zeolite. Actually, zeolites such as phillipsite, analcime, heulandite and clinoptilolite have been observed by the degradation of bentonite by high alkaline/pH solution at temperatures above 40 °C [14,15].

The chloride ingress at both interfaces, PC-OPA or PC-bentonite (e.g. [40,75,80,81]) is observed at 4–5 mm into the concrete and only little chloride is observed at the interface itself. The large gradient in chloride can be explained by the replacement of anions (OH-, sulphate of carbonate) in the AFm phases leading to the formation of Friedel's or Kuzel's salt [95]. This is also visualised for the simplified model in Fig. 2d, where Friedel's salt is modelled to precipitate at low OPA addition (few centimetres in the concrete) and destabilized at high addition (surface of the concrete). Although hydrotalcite is modelled, no uptake of chloride in the hydrotalcite is predicted. Chloride can also be sorbed by electrostatic interactions at the surface of C-S-H, compensating the positive apparent surface charge [56] and Cl/Si ratios in C-S-H up to ~0.2–0.3 have been observed by SEM/EDX [55,58]. Chloride uptake in C-S-H occurs preferentially at high Ca/Si [96,97], such that little chloride uptake at the interface is expected, where C-S-H is decalcified. The potential sorption of chloride by C-S-H was considered neither in the transport model (Fig. 7) nor in the simplified model (Fig. 2d).

Sulphur is concentrated in the cement near the interface (Fig. 6), which is similar to the seawater case discussed in Section 4.5 below. Ettringite precipitation has not been observed at the interface of Opalinus clay and Portland cement paste [74]. Some sulphate can also be bound by C-S-H with SO_4/Si (mol/mol) about 0.01–0.03, sulphate uptake is favoured at high Ca/Si in C-S-H [98]. Potentially, sulphate can be present in SO_4-hydrotalcite [38] or SO_4-AFm, although neither was predicted in the modelling. The simplified model in Fig. 2 predicts the phases observed experimentally but is not able to capture their spatial distribution as it does not account for transport of ions.

4.5. Seawater

The phase changes predicted by thermodynamic modelling in seawater are characterized by leaching at the near surface region (Fig. 2e), similar to the other solutions discussed above. In addition, experimental findings indicate a strong zonation for seawater exposed concretes as illustrated in Fig. 8 and in [5,57]. The relatively high sulphate, magnesium, and carbonate concentrations in the seawater (see Table 1), result in a zonation, forming calcite near the surface, followed by hydrotalcite, M-S-H, brucite and ettringite, and moving further into the concrete also an increased Friedel's salt formation is observed (Fig. 8 a). The zonation is independent of the exposure site (different salinity, temperature etc.) and the binder type used, as demonstrated in for a selection of the concretes investigated by Jakobsen et al. [4]. The same zonation has also been observed under deep-sea conditions [99] and it is

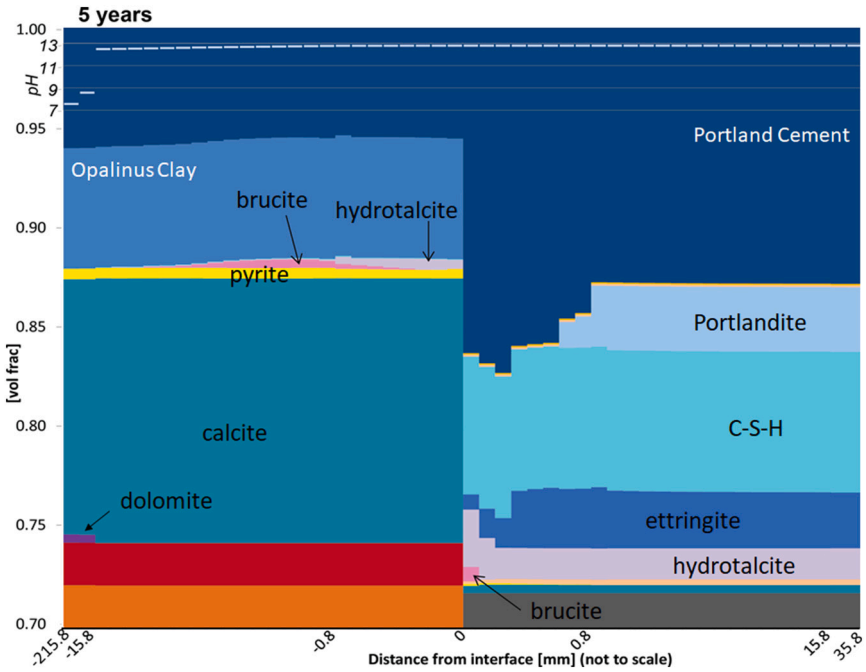

Fig. 7. Phases changes after 5 years at the interface between Opalinus clay and PC 2 (composition Table 2, w/c = 0.6) predicted by transport modelling. Adapted from [12].

similar to the ones observed by Duval and Hornain [100], Marchand et al. [101] and Chabrelie et al. [102]. Furthermore, it agrees rather well with the thermodynamic model (see Fig. 2e).

Seawater exposure leads to leaching of potassium and calcium near the surface. Consequently, a decrease in the portlandite content is observed. The extent of portlandite leaching depends on the calcium content of the binder and thereby the binder type as shown in [57]. The zone affected by leaching reaches deep into the concrete (see Fig. 8). At the surface of the concrete, brucite and calcium carbonate precipitate and can form a crust, if the samples are not exposed to strong abrasion on the concrete surface. Calcium carbonate can be present as calcite and aragonite [103]. Brucite and calcium carbonate are also found to precipitate in cracks that provide a direct path to the surface [5,104]. Such calcium carbonate and brucite crusts are also observed for mortars exposed to sea water under laboratory conditions, for example in Fig. 9 the crust is shown by a magnesium and calcium rich layer covering the surface [24].

The outermost couple of 100 μm up to about one millimetre of the cement paste are enriched in magnesium and low in chlorine and sulphur [57]. In this zone M-S-H had formed. This was not reported in [5], where the magnesium enrichment was attributed solely to brucite, while in a later study by the same authors, M(-A)-S-H with a Mg/Si molar ratio of approx. 1 and Al/Mg of 0.2 was identified in samples of hydrated cement paste flushed with sea water to simulate conditions for the outermost sections of the concrete [105]. The composition is within the range of M(-A)-S-H compositions observed in marine exposed concrete, i.e. 1–0.5 for Mg/Si and 0.05–0.3 for Al/Mg, as shown in [4,53], and agrees well with potential M(-A)-S-H compositions reported by Bernard et al. [106]. The presence of M-S-H and absence of C-S-H in this outermost zone would also indicate a pH in the range of 8–9 [107]. In fact, M-S-H formation is also predicted by modelling in the outermost zone as shown in Fig. 2 b). In the magnesium enriched zone, also carbonation is observed, which has been described as “popcorn” carbonation by Jakobsen et al. in [4] due to the specific morphology of the calcium carbonate.

The Mg-enriched zone is followed by a sulphur (most likely sulphate) enriched zone, which has a width from a couple of 100 μm to a couple of millimetres (see Fig. 8). In the sulphur zone, the precipitation of ettringite and thaumasite is observed in voids as shown in [4,5]. The presence of ettringite in the sulphur enriched zone indicates that the pH is above 10. Thaumasite ($Ca_3(SiO_3)(SO_4)(CO_3)\cdot 15H_2O$) forms from C-S-H in the presence of sulphate and carbonate and is faster at lower temperature than at ambient conditions [108]. Thaumasite formation is generally observed at temperatures between 5 and 15 °C [109,110], i.e. at a temperature range of sea water in moderate and cold climates [99]. The formation of thaumasite can, due to its low cementing properties, lead to disintegration and scaling of the concrete. It is important to note that although thaumasite and additional ettringite form, leading to an increase in the volume of the hydrates, typically no damage in the cement paste was observed in this zone [4]. The higher sulphur levels in this zone are accompanied by relatively low chloride levels [54]. The chloride content only increases once the sulphur content starts to decrease towards the background level of the cement paste.

Further in the concrete, the accumulation of chloride can be observed. In the case of the concrete exposed for 16 years, chloride accumulation has reached 40 mm (see Fig. 8). In agreement with these experimental observations, also the thermodynamic model predicts the formation of chloride containing AFm such as Friedel's salt instead of monocarbonate as illustrated in Fig. 2. The C(-A)-S-H will also take up some chlorides by physical binding [5,53–61], which is not considered in the thermodynamic model.

4.6. *Laboratory exposure to mixed sulphate solution in comparison with a bicarbonate containing mix solution*

The presence of sulphate in the interacting solution leads in the field to the secondary formation of ettringite, and possibly gypsum and thaumasite. Only a few studies are available which reported detailed data sets and most of those relate to the thaumasite form of deterioration [111–115]. The commonly suggested remedy is the use of dense cement pastes and curing that includes pre-carbonation [115]. Figg [115] provided a brief overview of the different sulphate sources ranging from soils containing salts, foundations or tunnels in contact with sulphate containing groundwaters, seawater, sewers and drains as well as

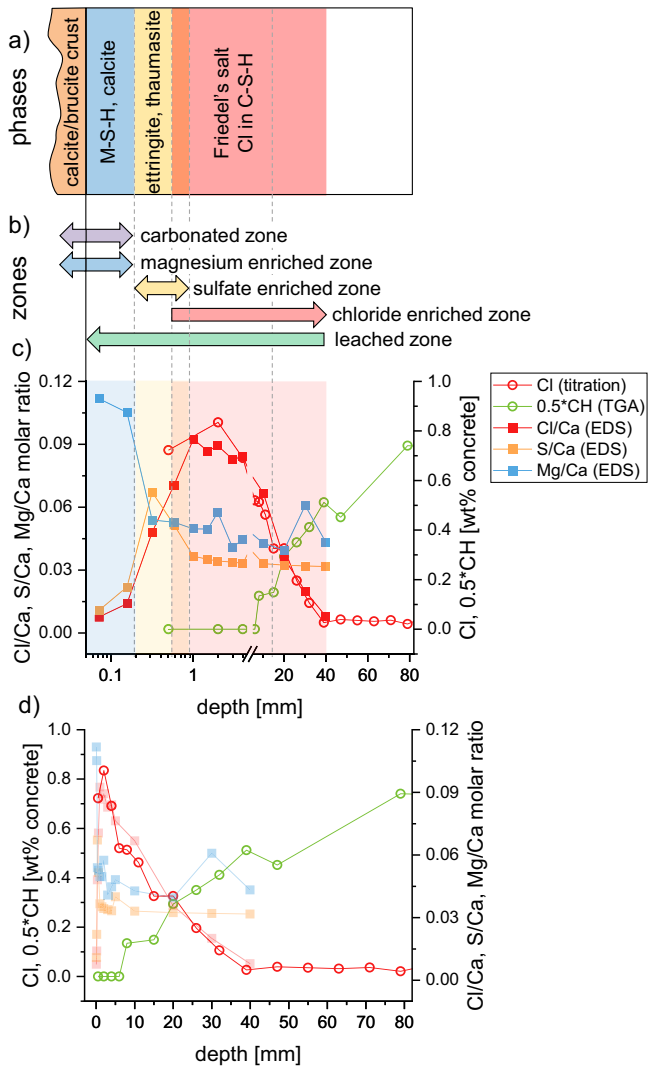

Fig. 8. a) Sketch illustrating the main phases which form upon marine exposure; b) Illustration of the zones; c) and d) the total chloride and portlandite (CH) profiles, as well as Cl/Ca, S/Ca and Mg/Ca profiles as molar ratio for a concrete element exposed submerged in sea water at Solsvik field station for 16 years. The concrete was made with a Portland composite cement containing 4 % silica fume and 19 % fly ash. Note that the horizontal axis is split in a logarithmic part up to 4 mm and a linear part from 4 to 82 mm. d) The same data as in c) where the horizontal axis is linear, and the vertical axes are swopped. This to illustrate that the elemental changes caused by sulphur and magnesium only affect the outer millimetres, whereas the portlandite (CH) and chloride change over a larger depth. For more information see [57].

sulphide containing aggregates.

Most publications focus not on field samples, but on simplified tests using Na_2SO_4 or $MgSO_4$ solutions. A wide range of experimental factors have an influence on the response of the test set-up; amongst others: cement type, mix-design, sulphate concentration, relation between the liquid volume and volume and composition of the sample, exchange frequency, temperature etc. as discussed in [27,116–118]. Sodium sulphate is used for laboratory testing to maximise the formation of ettringite and gypsum, which depend on the sulphate concentration [119]; while the chemical binding of sodium is not documented in the related literature, except for very high concentrations [120,121]. The second most used salt is magnesium sulphate, which leads to the precipitation of brucite and, especially for the case of low Ca/Si ratio binders [122], the formation of M-S-H phases is often observed together with hydrotalcite/LDH [123]. Aqueous exposure solutions containing several ions show reduced expansions compared to single salt solutions, which appears to be even more pronounced for competing anions such as sulphates and bicarbonates [27,124,125], while the simultaneous presence of sulphates and chlorides yield contradicting results [126,127].

Laboratory studies containing i) mixtures of sulphate salts (K, Na, Mg and Ca-sulphate) and ii) mixtures containing additionally bicarbonate ions to mimic field conditions (Table 1) results in a succession of zones as well as leaching. The simplified modelling in Fig. 2f predicts for the "sulphate solution", a mixture of Na_2SO_4, K_2SO_4, $MgSO_4$ and $CaSO_4$ $2H_2O$ (molar sulphate ratio of 3:1:2:2) with a sulphate content of 50 g/L as often used in accelerated tests, Table 1, an increase of ettringite towards the surface that is accompanied by the dissolution of portlandite and the present AFm and LDH type phases. In surface proximity, the only stable phases are gypsum, M-S-H, brucite and hydrotalcite. For the "bicarbonate solution", which contains equal amounts of sulphate as the sulphate solution plus sodium bicarbonate (Table 1), the calculated precipitation of ettringite (Fig. 2g) is accompanied by the massive precipitation of calcite from the exposure solution. In addition, the formation of smaller quantities of M-S-H, brucite, hydrotalcite and a zeolitic phase (Na-chabazite) is predicted.

Fig. 10 to Fig. 12 highlight different details observed experimentally on Portland mortars exposed to the sulphate and bicarbonate solution; experiments and cement compositions are detailed in [28]. Fig. 10 shows the changes in CaO and SO_3 as a function of depth from the exposed surface for exposure to the sulphate mixture and the bicarbonate mixture. The exposure to the sulphate mixture solution leads to the formation of gypsum in surface proximity which is coupled with leaching of calcium from the binder; see Fig. 10 and Fig. 11 a). At greater depths (> 2 mm) the high CaO values indicate the presence of portlandite. The CaO contents are lowest where the sulphate contents are highest, which is where gypsum is the dominating phase. On the surface, CaO contents increase again due to a limited carbonation of the sample surface. The highest sulphate concentrations are observed in surface proximity for the sulphate mixture solution. Further inside the sample, ettringite is formed and the sulphate content (moving average of the data points) reduces up to 6.5–7.0 mm where it matches the background values.

For the bicarbonate mixture solution, neither CaO nor sulphate contents seem to be affected. The formation of $CaCO_3$ in the microstructure leads to similar CaO contents as for portlandite. The sulphate contents are clearly lowered in the presence of bicarbonate. The simplified modelling predictions (Fig. 2g) indicate that the precipitation of calcite reduces the availability of calcium necessary to form ettringite, consistent with limited amount of secondary ettringite formation observed in Fig. 10 and Fig. 11b. The suppression of ettringite formation by sodium bicarbonate is consistent with the observations for solutions consisting only of Na_2SO_4 or $MgSO_4$, and with thermodynamic modelling [124,125] and underlines the importance of bicarbonate ions to reduce sulphate binding. This is also demonstrated by the low SO_3 contents in the carbonated zone (with almost no variation) in Fig. 10. The additional formation of ettringite behind the carbonated zone, which is predicted by the simplified model (Fig. 2g), is not visible in Fig. 10.

Analysing the smoothed CaO and SO_3 median values in Fig. 10 shows that the CaO profile for the sulphate exposure (blue line) is slowly reducing from ca. 55 mass % to 40 mass %, between 0.0 and 2.5 mm. This indicates the leaching of the C-S-H phases towards the surface. On the contrary, the median values are not affected for the sample exposed to the bicarbonate solution, where calcium carbonate has formed, such that the extent of affected zones cannot be clearly assessed. For low Ca/Si binders, such as slag cements, the extent of the affected zone in the presence of bicarbonate has been more pronounced for simultaneous exposure to sulphate and bicarbonate ions [124,125].

Brucite, which precipitates readily for PC binders exposed to magnesium sulphate containing exposure conditions, is predicted and

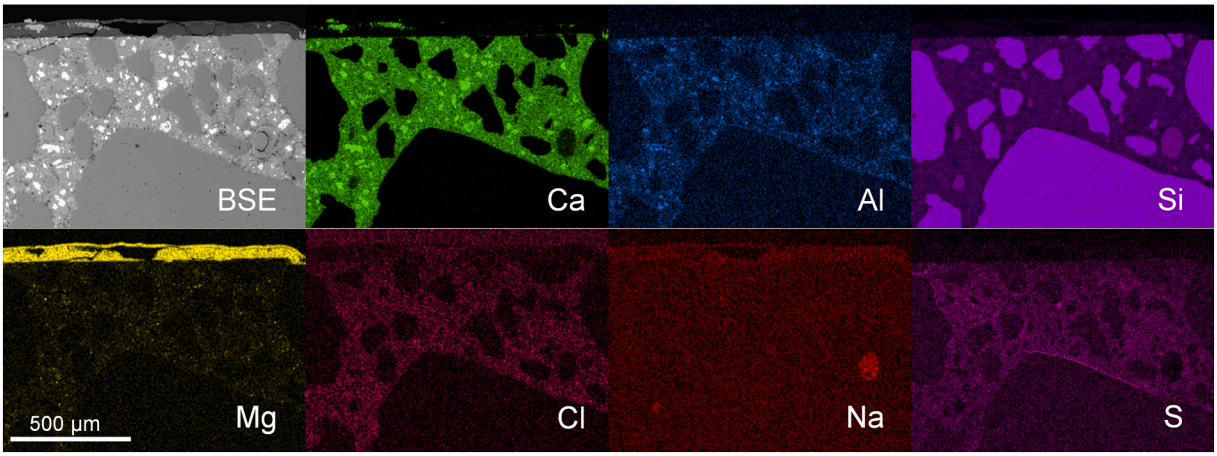

Fig. 9. Elemental maps of the laboratory exposed surface of Portland cement mortar exposed to sea water for 90 days. The exposed surface is at the top of the images. For more information see [24].

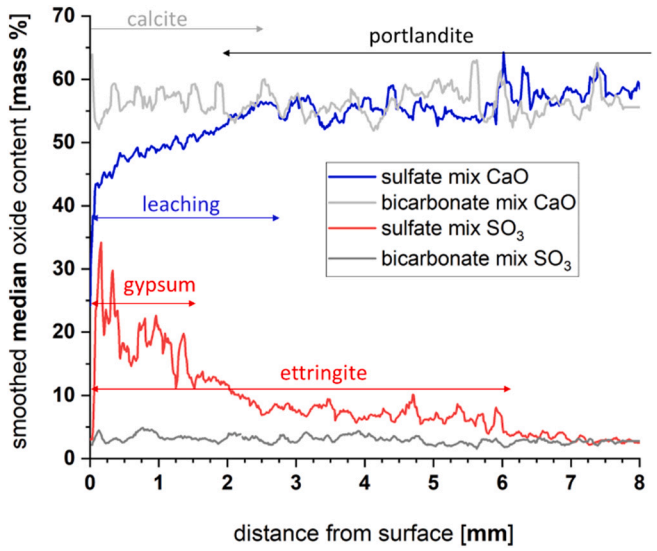

Fig. 10. CaO and SO_3 median profiles for Portland cement mortars exposed for 637 days (colored) to sulphate mixture and one year to the bicarbonate mixture solution (grey lines). For experimental details see [28].

observed for the sulphate solution (Fig. 12a), while the other magnesium containing phases (M-S-H, hydrotalcite) are not clearly detected. In contrast, the sample exposed to the bicarbonate mixture solution does not show a distinct MgO rich surface zone (Fig. 12b), while there might be a confined enrichment in Na_2O and K_2O in surface proximity, although the levels of alkalis are low. K_2O seems to be slightly more increased, which could point towards the formation of zeolitic phases such as the chabazite predicted by the simplified model (Fig. 2g).

Overall, the data and modelling show that the carbonation of cementitious binders can prevent the leaching of calcium from the binders, as the calcium is bound in calcium carbonate and thus not available to form other hydrate phases. The strong binding of calcium by calcium carbonate resulted in a much lower expansion of the samples exposed to the bicarbonate solution than of the samples exposed to the sulphate solution, although the sulphate content of the solutions was identical. This illustrates how lowering the availability of calcium can lower the potential for deleterious ettringite formation, especially over long time periods. The lowering of ettringite formation observed and modelled here in the presence of bicarbonate, also supports the observations that carbonation during curing (before exposure) improves the sulphate resistance of concrete [115].

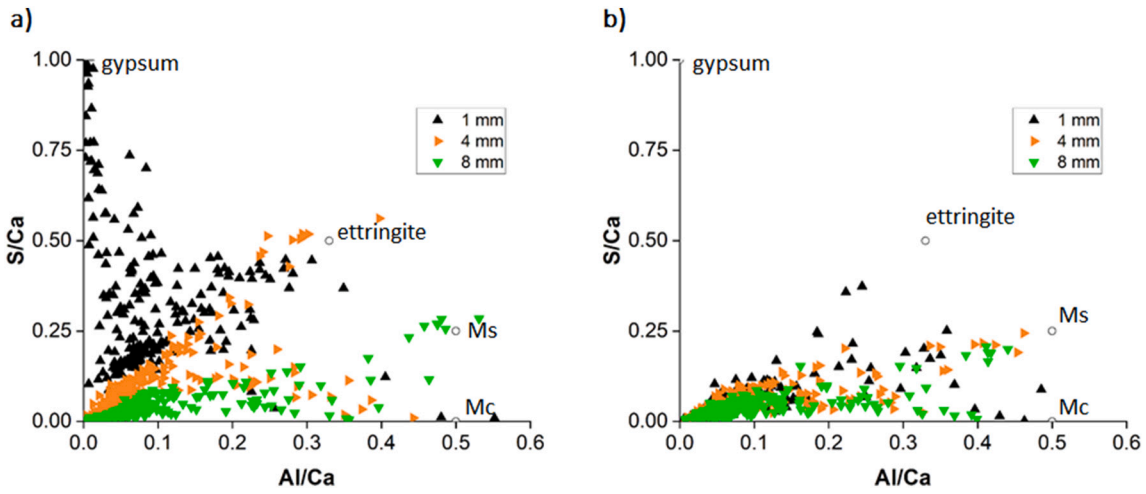

Fig. 11. Atomic ratio plots for three key depths, corresponding to the profiles shown in Fig. 10, for both exposure conditions a) with a sulphate content of 350 mM, and b) the bicarbonate mixture solution that contains the same sulphate salts proportions and quantities in addition to 350 mM $NaHCO_3$. Ms. = monosulphate, Mc = monocarbonate. For experimental details see [28].

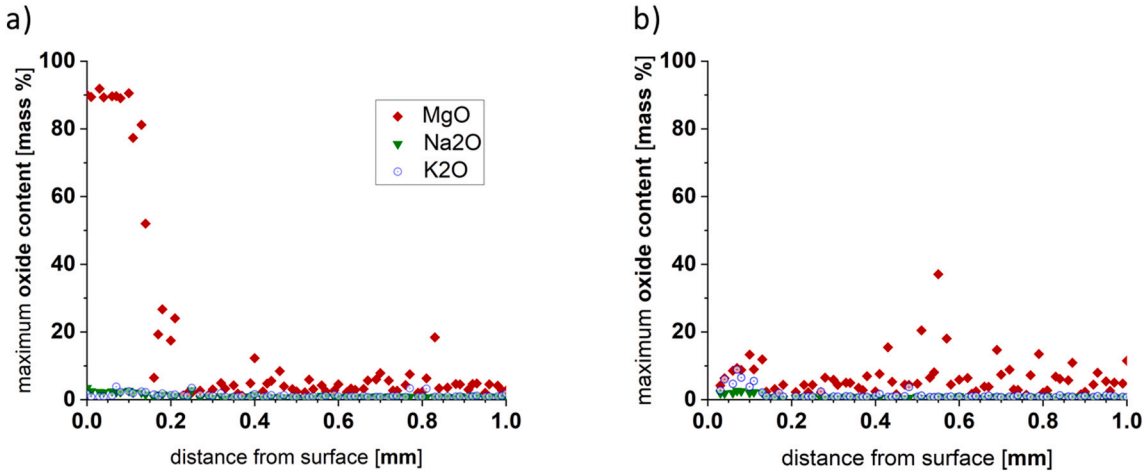

Fig. 12. MgO, Na_2O and K_2O profiles for the highest values per distance measured, for the PC mortars exposed to a) sulphate mixture for 637 days; and b) bicarbonate mixture solution for 364 days. For experimental details see [28].

4.7. Comparison of the effect of solution composition

The investigations of the changes at the surface of cement paste, mortar and concrete detailed above indicate that in many cases leaching is the dominant underlying degradation mechanism. The extent of leaching depends on the solution composition. In natural environments, in particular the concentration of sulphate and (bi)carbonate greatly affects the portlandite leaching as illustrated in Fig. 13a). The simplified modelling illustrates how the calculated portlandite leaching front moves inward to the cement paste as a function of the sum of the sulphate and carbonate concentrations: river, NaCl and granite (<1 to 3 mM) < saline clay (16–22 mM) and seawater (31 mM) < sulphate solution with 352 mM < bicarbonate solution with a total of 702 mM SO_4 + HCO_3. Sulphate and carbonate in solution contribute to the destabilisation of portlandite due to their strong tendency to form solid Ca-containing phases making their presence a major driver for calcium leaching from the cement:

$$Ca(OH)_2 + SO_4^{2-} + 2H_2O \Rightarrow CaSO_4{\cdot}2H_2O(\text{gypsum}) + 2OH^- \quad (1)$$

$$Ca(OH)_2 + CO_3^{2-} \Rightarrow CaCO_3(\text{calcite}) + 2OH^- \quad (2)$$

Eqs. (1) and (2) illustrate that the formation of gypsum and calcite not only destabilises portlandite (or other Ca-rich hydrates) but also releases hydroxyl ions, increasing the pH values near the interface as also visible in the calculated pH values (Fig. 13b) in the region where portlandite leaches.

Nearer to the surface, however, this effect is no longer visible and the buffering capacity of the interacting solution dominates the calculated pH values. High pH values are calculated for solutions with a low buffering capacity such as river and granite water and NaCl solution, where the pH values are dominated by the leaching of alkalis from the cement. For the solutions richer in carbonate and Mg-containing solutions, pH values around 10 are predicted, as they are buffered strongly by the formation of calcite, brucite and M-S-H. The lowest pH values were calculated for $NaHCO_3$ solution, which forms a strong buffer towards pH 6.

As mentioned earlier, an increase of KOH concentrations in exposure solutions limited the observed leaching of portlandite strongly [68,128], as also shown in Fig. 14b. This was explained by the reduction in the leaching potential of calcium from the cement paste in a high pH exposure solution. Increasing the hydroxyl concentration in the exposure solution was also observed to slow down the ingress of ions such as chloride (see Fig. 14a), thereby indicating a strong link between leaching and ingress of ions [68,128].

The formation of a dense surface layer due to precipitation of calcite, brucite or additional ettringite can lead to a local reduction in the porosity which might be expected to reduce the ingress of ions or leaching from the cement paste. High carbonate concentrations have shown to reduce the porosity due to calcium carbonate formation in calcium rich cements, limiting the ingress of for example sulphates and slowing down or even preventing damage due to ettringite formation [27,124,125]. High sulphate concentrations without carbonates are more problematic as they lead to expansion, spalling/softening and cracking and thus to opening of "highways" for the ingress of other ions

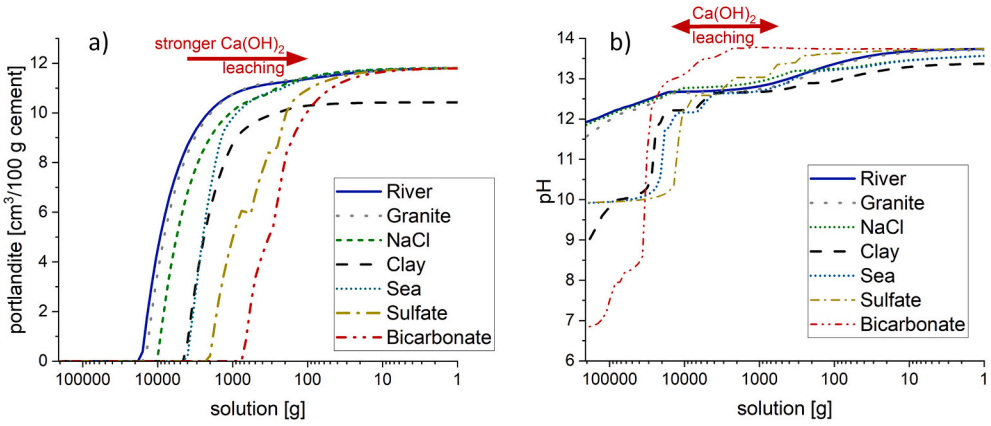

Fig. 13. a) Modelled effect of solution composition on a) portlandite leaching and b) calculated pH values of the exposure solution in equilibrium with the solids.

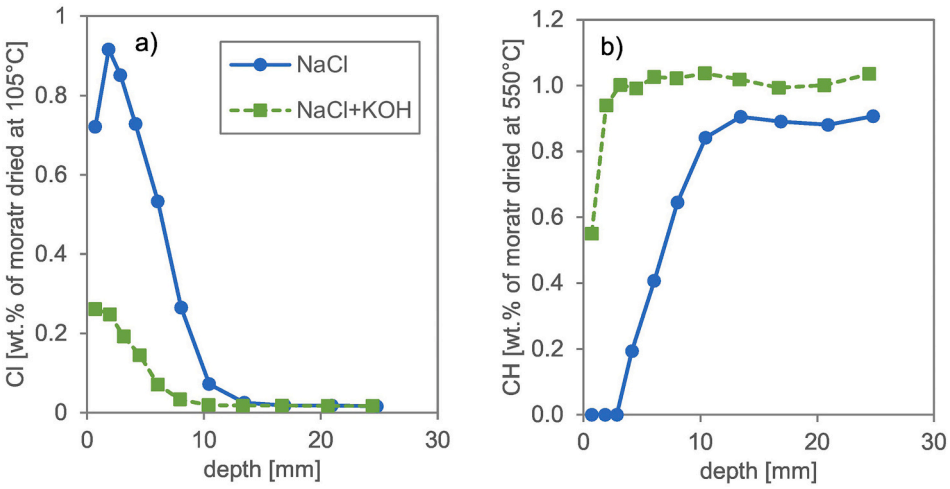

Fig. 14. a) Total chloride profiles for mortar specimens with a w/b ratio of 0.43 and prepared with a CEM VI (SV) Portland composite cement containing fly ash and slag precured for 76 days and then exposed to 3 % NaCl or 3 % NaCl +0.8 % KOH solution for 180 days. The chloride content was determined on the profile ground sections with increasing depth from the exposed surface using potentiometric titration, b) Portlandite (CH) profiles determined on the same batch of profile ground mortar powder using TGA. Adapted from [128].

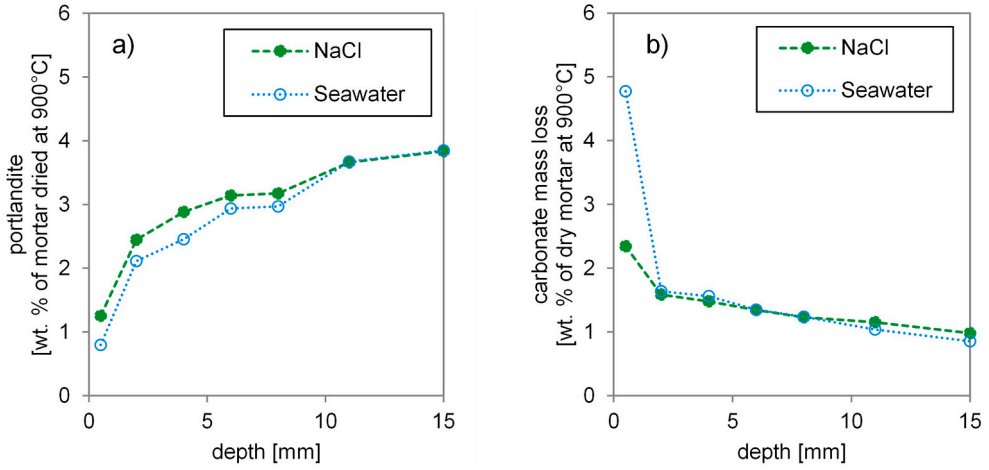

Fig. 15. a) Measured portlandite destabilisation and b) calcite formation after 180 days of exposure to seawater or NaCl solution with the same chloride concentration, adapted from [24].

and a faster degradation. In contrast, simple laboratory experiments comparing chloride ingress for seawater exposure with NaCl solution exposure showed that the formation of a seemingly dense magnesium and calcium carbonate layer in the case of seawater did not slow down the chloride ingress nor the leaching [24]. To the contrary, a slightly higher chloride ingress and leaching was observed for seawater exposed mortar compared to the ones exposed to NaCl solution (see Fig. 15). This is in line with the findings from Rosenqvist et al. [16], who observed a dense calcite rich layer at the surface, which did not prevent the deeper laying zones from being heavily leached. These observations illustrate that the effect of the formation of additional phases can be very divers and complex such that no direct simple correlation between solid volume, porosity and transport can be derived.

5. Conclusions

We have focussed on the impact of fresh water and multi-component saline solutions on the long-term changes in the phase assemblage in Portland cement-based cementitious materials. The comparison of detailed studies of long-term changes observed on field exposed concrete, with laboratory exposed samples, and with transport modelling available in literature gave a coherent picture of the effect of the different investigated solutions. In addition, a simplified thermodynamic modelling approach was used to calculate the effect of solution composition on the intensity of leaching and on the kind and quantity of phases formed at the interface with the environment. Note porosity, pore structure and interfacial transition zone could also significantly affect the transport which has not been addressed in the current paper.

The saline solutions investigated include fresh water, NaCl solutions, rock and clayey water, seawater and sulphate containing solutions.

The comparison of the experimental observations collected from literature with the simplified modelling approach allowed to identify the following main effects on hydrate cement pastes caused by the environment:

- A main underlying degradation mechanism for cement paste exposed to the investigated solutions is leaching as illustrated in Fig. 2 as well as in the sketches presented in Fig. 16
- The leaching is amongst others reflected in the portlandite depletion (Fig. 13) as well as in the decomposition of calcium containing phases such as AFm and AFt phases, followed by the decalcification and finally the decomposition of C(-A)-S-H as illustrated in Fig. 16

The solution composition as well as its availability determined the extent of leaching, the kind and quantity of phases formed as well as the

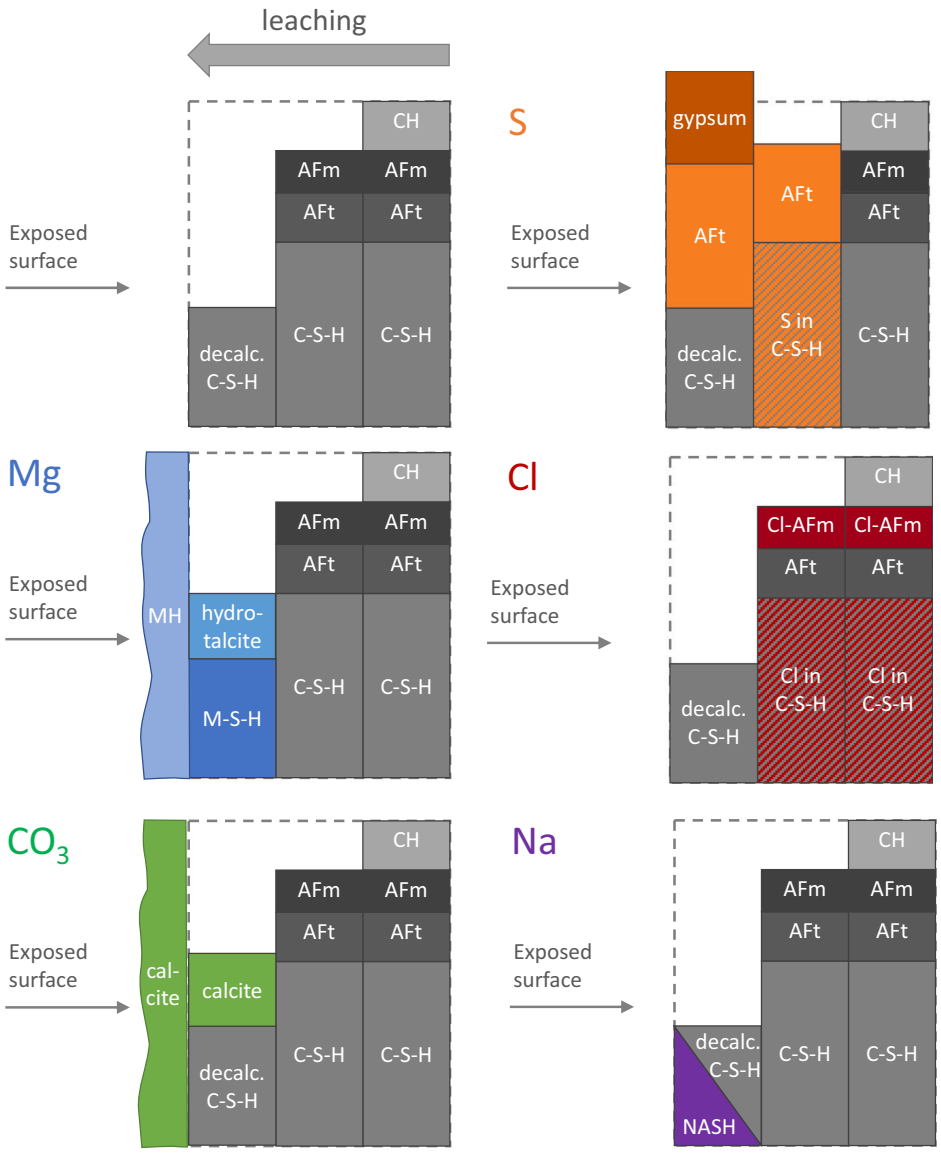

Fig. 16. Summary sketch very simply illustrating the impact of leaching on the phase assemblage, as well as how individual ions in the exposure solution cause phase changes.

pH values in the interface and its proximity. The presence of carbonate and sulphate in the interaction solution accelerates the leaching of Ca-rich hydrates as shown in Fig. 13, due to the formation of calcite and gypsum or ettringite, which destabilises Ca-rich phases such as portlandite and C-S-H.

The type and concentrations of other elements in the exposure solution determine which phases will precipitate at the interface of the cement with the environment as illustrated in Fig. 16. Generally, the following order can be observed from the unaffected core towards the interface with the solution:

- Chloride ingresses relatively far into the cement paste and leads at increased concentrations (> 100 mM) to the formation of chloride containing AFm phases (Friedel's or Kuzel's salt), which form at the expense of other AFm phases such as monosulphate or monocarbonate, leading to little alteration in the microstructure. In addition, chlorides can accumulate through physical binding in C-S-H.
- The presence of sulphate leads to the formation of ettringite, gypsum at very high sulfate concentrations and in the long-term, and in the presence of carbonates also to thaumasite. The formation of these phases leads to an increase in the volume of the solids and potentially spalling and cracking of the concrete if formed in high amounts. Whether macroscopic damage occurs depends strongly on the amount and location of ettringite and thaumasite formation. In low quantities as e.g. observed at the interface with clay or seawater, the formation of ettringite and/or thaumasite does not lead to macroscopic damage as at the same time leaching occurs. The effect of sulphate is much stronger in high sulphate containing solutions such as the pore water of gypsum containing clays or rocks, leading to cracking, spalling or complete deterioration of the concrete at its surface.
- The content of carbonate and bicarbonate in the interacting solutions determines the amount of calcium carbonate formed at the interface or in the surrounding environment. At high carbonate concentrations, the precipitation of carbonate can suppress ettringite formation as it limits the availability of calcium.
- Magnesium as present in granitic, clay and sea water results in the formation of M-S-H, hydrotalcite and brucite, depending on the Mg concentration, the availability of Si and Al and pH values. These

phases are generally observed as a crust at the interface with little mechanical strength.
- Sodium and potassium in the solution can lead to the formation of zeolitic phases (NASH or KASH phases) at the extreme decalcified surface. They are, however, difficult to detect.

In conclusion, the ions in the exposure solutions, i.e. chloride, sulphate, carbonates, magnesium and sodium and potassium, do not necessarily have a detrimental impact on the cement paste, except for high sulphate solutions. In saturated conditions it is mainly their effect on leaching, the underlying degradation mechanism for all investigated exposure solutions, which determines the progress of the degradation and thereby determines the service life of the affected concrete. In other words, the leaching resistance of a cement paste is a crucial performance indicator for concrete in contact with multi-component solutions. The leaching resistance of a concrete could be tested with fresh water, as the other ions (except for high sulphate concentrations) do not appear to play a major role.

It should be noted that under non-saturated conditions secondary effects such as drying and wick-action can lead to much higher salt concentrations and substantial damage by physical effects such as crystallization.

CRediT authorship contribution statement

Klaartje De Weerdt: Investigation, Writing – original draft, Writing – review & editing, Visualization. **Ellina Bernard:** Investigation, Writing – original draft, Writing – review & editing, Visualization. **Wolfgang Kunther:** Investigation, Writing – original draft, Writing – review & editing, Visualization. **Malene Thostrup Pedersen:** Investigation, Writing – original draft, Writing – review & editing, Visualization. **Barbara Lothenbach:** Software, Investigation, Writing – original draft, Writing – review & editing, Visualization, Supervision.

Declaration of competing interest

The authors declare that they have no known competing financial interests or personal relationships that could have appeared to influence the work reported in this paper.

Data availability

Data will be made available on request.

Acknowledgments

The financial support of the Swiss National Science Foundation (SNSF) for Ellina Bernard's Postdoc mobility under the grant P400P2_194345 is gratefully acknowledged as well as helpful discussions with Andreas Jenni and Urs Mäder.

References

[1] M. Alexander, A. Bertron, N.De Belie, Performance of cement-based materials in aggressive aqueous environments, in: State-of-the-Art Report, RILEM TC 211 - PAE, Springer, 2013.
[2] W. Stumm, J.J. Morgan, Aquatic Chemistry. Chemical Equilibria and Rates in Natural Waters, 3rd ed., John Wiley & Sons, Inc., New York, 1996.
[3] M. Mazurek, P. Alt-Epping, A. Bath, T. Gimmi, H.N. Waber, S. Buschaert, P. De Cannière, M. De Craen, A. Gautschi, S. Savoye, Natural tracer profiles across argillaceous formations, Appl. Geochem. 26 (2011) 1035–1064.
[4] U.H. Jakobsen, K. De Weerdt, M.R. Geiker, Elemental zonation in marine concrete, Cem. Concr. Res. 85 (2016) 12–27.
[5] K. De Weerdt, H. Justnes, M.R. Geiker, Changes in the phase assemblage of concrete exposed to sea water, Cem. Concr. Compos. 47 (2014) 53–63.
[6] B. Lothenbach, F. Winnefeld, Thermodynamic modelling of the hydration of Portland cement, Cem. Concr. Res. 36 (2006) 209–226.
[7] A. Vollpracht, B. Lothenbach, R. Snellings, J. Haufe, The pore solution of blended cements: a review, Mater. Struct. (2015) 1–27.
[8] M. Adler, U. Mäder, H.N. Waber, High-pH alteration of argillaceous rocks: an experimental study, Schweiz. Mineral. Petrogr. Mitt. 79 (1999) 445–454.
[9] F. Claret, A. Bauer, T. Schäfer, L. Griffault, B. Lanson, Experimental investigation of the interaction of clays with high-pH solutions: A case study from the Callovo-Oxfordian formation, Meuse-Haute Marne underground laboratory (France), Clays and Clay Minerals 50 (2002) 633–646.
[10] S. Ramírez, J. Cuevas, R. Vigil, S. Leguey, Hydrothermal alteration of "La Serrata" bentonite (Almeria, Spain) by alkaline solutions, Applied Clay Science 21 (2002) 257–269.
[11] A. Bauer, G. Berger, Kaolinite and smectite dissolution rate in high molar KOH solutions at 35 and 80 C, Appl. Geochem. 13 (1998) 905–916.
[12] A. Jenni, T. Gimmi, P. Alt-Epping, U. Mäder, V. Cloet, Interaction of ordinary Portland cement and Opalinus Clay: Dual porosity modelling compared to experimental data, Phys. Chem. Earth, Parts A/B/C 99 (2017) 22–37.
[13] A. Dauzères, P.Le Bescop, P. Sardini, C.Cau Dit Coumes, Physico-chemical investigation of clayey/cement-based materials interaction in the context of geological waste disposal: Experimental approach and results, Cement and Concrete Research 40 (2010) 1327–1340.
[14] E.C. Gaucher, P. Blanc, Cement/clay interactions–a review: experiments, natural analogues, and modeling, Waste Manag. 26 (2006) 776–788.
[15] D. Savage, C. Walker, R. Arthur, C. Rochelle, C. Oda, H. Takase, Alteration of bentonite by hyperalkaline fluids: a review of the role of secondary minerals, Phys. Chem. Earth, Parts A/B/C 32 (2007) 287–297.
[16] M. Rosenqvist, A. Bertron, K. Fridh, M. Hassanzadeh, Concrete alteration due to 55years of exposure to river water: chemical and mineralogical characterisation, Cem. Concr. Res. 92 (2017) 110–120.
[17] U.K. Mäder, T. Fierz, B. Frieg, J. Eikenberg, M. Rüthi, Y. Albinsson, A. Möri, S. Ekberg, P. Stille, Interaction of hyperalkaline fluid with fractured rock: Field and laboratory experiments of the HPF project (Grimsel Test Site, Switzerland), Journal of Geochemical Exploration 90 (2006) 68–94.
[18] J.L. Garcia Calvo, A. Hidalgo, C. Alonso, L. Fernández Luco, Development of low-pH cementitious materials for HLRW repositories: resistance against ground waters aggression, Cem. Concr. Res. 40 (2010) 1290–1297.
[19] J. Tremosa, D. Arcos, J. Matray, F. Bensenouci, E.C. Gaucher, C. Tournassat, J. Hadi, Geochemical characterization and modelling of the Toarcian/Domerian porewater at the tournemire underground research laboratory, Appl. Geochem. 27 (2012) 1417–1431.
[20] E. Gaucher, C. Lerouge, Caractérisation géochimique des forages PAC et nouvelles modélisations THERMOAR, in: BRGM Reports, 2007.
[21] P. Wersin, M. Pekala, M. Mazurek, T. Gimmi, U. Mäder, A. Jenni, D. Rufer, AL, Porewater chemistry of opalinus clay: methods, data, modelling & buffering capacity, in: NTB 18-01, 2021.
[22] A.M. Fernández, B. Baeyens, M. Bradbury, P. Rivas, Analysis of the porewater chemical composition of a Spanish compacted bentonite used in an engineered barrier, Phys. Chem. Earth, Parts A/B/C 29 (2004) 105–118.
[23] A.D. Herholdt, C.F. Justesen, P. Nepper-Christensen, N.A. Betong-bogen, The Concrete Book 2, 1985.
[24] K. De Weerdt, B. Lothenbach, M.R. Geiker, Comparing chloride ingress from seawater and NaCl solution in Portland cement mortar, Cem. Concr. Res. 115 (2019) 80–89.
[25] A. Demayo, Elements in sea water, in: D.R. Lide (Ed.), CRC Handbook of Chemistry and Physics, CRC Press U.S.A, 1992.
[26] F.J. Millero, R. Feistel, D.G. Wright, T.J. McDougall, The composition of standard seawater and the definition of the reference-composition salinity scale, Deep-Sea Res. I Oceanogr. Res. Pap. 55 (2008) 50–72.
[27] W. Kunther, B. Lothenbach, K. Scrivener, On the relevance of volume increase for the length changes of mortar bars in sulfate solutions, Cem. Concr. Res. 46 (2013) 23–29.
[28] W. Kunther, Investigation of Sulfate Attack by Experimental and Thermodynamic Means, EPFL Lausanne, Switzerland, 2012. PhD thesis.
[29] K. De Weerdt, M.B. Haha, G. Le Saout, K.O. Kjellsen, H. Justnes, B. Lothenbach, Hydration mechanisms of ternary Portland cements containing limestone powder and fly ash, Cem. Concr. Res. 41 (2011) 279–291.
[30] R. Loser, B. Lothenbach, A. Leemann, M. Tuchschmid, Chloride resistance of concrete and its binding capacity – comparison between experimental results and thermodynamic modeling, Cem. Concr. Compos. 32 (2010) 34–42.
[31] B. Lothenbach, B. Bary, P. Le Bescop, T. Schmidt, N. Leterrier, Sulfate ingress in Portland cement, Cem. Concr. Res. 40 (2010) 1211–1225.
[32] D. Kulik, T. Wagner, S. Dmytrieva, G. Kosakowski, F. Hingerl, K. Chudnenko, U. Berner, GEM-selektor geochemical modeling package: revised algorithm and GEMS3K numerical kernel for coupled simulation codes, Comput. Geosci. 17 (2013) 1–24.
[33] T. Thoenen, W. Hummel, U. Berner, E. Curti, The PSI/Nagra Chemical Thermodynamic Database 12/07, PSI Report 14–04, Villigen PSI, Switzerland, 2014.
[34] B. Lothenbach, D.A. Kulik, T. Matschei, M. Balonis, L. Baquerizo, B. Dilnesa, G. D. Miron, R.J. Myers, Cemdata18: a chemical thermodynamic database for hydrated Portland cements and alkali-activated materials, Cem. Concr. Res. 115 (2019) 472–506.
[35] B. Ma, B. Lothenbach, Thermodynamic study of cement/rock interactions using experimentally generated solubility data of zeolites, Cem. Concr. Res. 135 (2020), 106149.
[36] B. Ma, B. Lothenbach, Synthesis, characterization, and thermodynamic study of selected na-based zeolites, Cem. Concr. Res. 135 (2020), 106111.
[37] B. Ma, B. Lothenbach, Synthesis, characterization, and thermodynamic study of selected K-based zeolites, Cem. Concr. Res. 148 (2021), 106537.

[38] E. Bernard, J. Zucha, B. Lothenbach, U. Mäder, Stability of hydrotalcite (Mg-Al double layer hydroxide) in presence of different anions, Cem. Concr. Res. 152 (2022), 106674.
[39] D.A. Kulik, Improving the structural consistency of C-S-H solid solution thermodynamic models, Cem. Concr. Res. 41 (2011) 477–495.
[40] E. Bernard, A. Jenni, N. Toropovs, U. Mäder, Percolation experiment with 10-year-old interface between Opalinus Clay and Portland concrete, Cement and Concrete Research, submitted.
[41] E. Wieland, B. Lothenbach, M. Glaus, T. Thoenen, B. Schwyn, Influence of superplasticizer on the long-term properties of cements and possible impacts on radionuclide uptake in cement based repository for radioactive waste, Appl. Geochem. 49 (2014) 126–142.
[42] B. Lothenbach, G. Le Saout, E. Gallucci, K. Scrivener, Influence of limestone on the hydration of Portland cements, Cem. Concr. Res. 38 (2008) 848–860.
[43] B. Lothenbach, K. Scrivener, R.D. Hooton, Supplementary cementitious materials, Cem. Concr. Res. 41 (2011) 1244–1256.
[44] S.J. Mills, A.G. Christy, J.-M. Génin, T. Kameda, F. Colombo, Nomenclature of the hydrotalcite supergroup: natural layered double hydroxides, Mineral. Mag. 76 (2012) 1289–1336.
[45] I.G. Richardson, Clarification of possible ordered distributions of trivalent cations in layered double hydroxides and an explanation for the observed variation in the lower solid-solution limit, Acta Crystallogr. Sect. B: Struct. Sci. Cryst. Eng. Mater. 69 (2013) 629–633.
[46] K. Rozov, U. Berner, D. Kulik, L.W. Diamond, Solubility and thermodynamic properties of carbonate-bearing hydrotalcite–pyroaurite solid solutions with a 3: 1 Mg/(Al+ Fe) mole ratio, Clay Clay Miner. 59 (2011) 215–232.
[47] K. Rozov, U. Berner, C. Taviot-Gueho, F. Leroux, G. Renaudin, D. Kulik, L. W. Diamond, Synthesis and characterization of the LDH hydrotalcite–pyroaurite solid-solution series, Cem. Concr. Res. 40 (2010) 1248–1254.
[48] A. Jenni, U. Mäder, C. Lerouge, S. Gaboreau, B. Schwyn, In situ interaction between different concretes and opalinus clay, Phys. Chem. Earth, Parts A/B/C 70 (2014) 71–83.
[49] P. Faucon, F. Adenot, M. Jorda, R. Cabrillac, Behaviour of crystallised phases of Portland cement upon water attack, Mater. Struct. 30 (1997) 480–485.
[50] P. Faucon, F. Adenot, J.F. Jacquinot, J.C. Petit, R. Cabrillac, M. Jorda, Long-term behaviour of cement pastes used for nuclear waste disposal: review of physico-chemical mechanisms of water degradation, Cem. Concr. Res. 28 (1998) 847–857.
[51] D. Nied, K. Enemark-Rasmussen, E. L'Hôpital, J. Skibsted, B. Lothenbach, Properties of magnesium silicate hydrates (M-S-H), Cement and Concrete Research 79 (2016) 323–332.
[52] C. Roosz, S. Grangeon, P. Blanc, V. Montouillout, B. Lothenbach, P. Henocq, E. Giffaut, P. Vieillard, S. Gaboreau, Crystal structure of magnesium silicate hydrates (MSH): the relation with 2: 1 Mg–Si phyllosilicates, Cem. Concr. Res. 73 (2015) 228–237.
[53] K. De Weerdt, H. Justnes, U.H. Jakobsen, M.R. Geiker, M-S-H Formation in Marine Exposed Concrete, ICCCBeijng, China, 2015.
[54] K. De Weerdt, D. Orsáková, M.R. Geiker, The impact of sulphate and magnesium on chloride binding in Portland cement paste, Cem. Concr. Res. 65 (2014) 30–40.
[55] K. De Weerdt, A. Colombo, L. Coppola, H. Justnes, M.R. Geiker, Impact of the associated cation on chloride binding of Portland cement paste, Cem. Concr. Res. 68 (2015) 196–202.
[56] G. Plusquellec, A. Nonat, Interactions between calcium silicate hydrate (C-S-H) and calcium chloride, bromide and nitrate, Cem. Concr. Res. 90 (2016) 89–96.
[57] K. De Weerdt, D. Orsáková, A.C.A. Müller, C.K. Larsen, B. Pedersen, M.R. Geiker, Towards the understanding of chloride profiles in marine exposed concrete, impact of leaching and moisture content, Constr. Build. Mater. 120 (2016) 418–431.
[58] A. Machner, M. Zajac, M. Ben Haha, K.O. Kjellsen, M.R. Geiker, K. De Weerdt, Chloride-binding capacity of hydrotalcite in cement pastes containing dolomite and metakaolin, Cem. Concr. Res. 107 (2018) 163–181.
[59] Z. Shi, M.R. Geiker, K. De Weerdt, T.A. Østnor, B. Lothenbach, F. Winnefeld, J. Skibsted, Role of calcium on chloride binding in hydrated Portland cement–metakaolin–limestone blends, Cem. Concr. Res. 95 (2017) 205–216.
[60] K. De Weerdt, Chloride binding in concrete: recent investigations and recognised knowledge gaps: RILEM Robert L'Hermite medal paper 2021, Mater. Struct. 54 (2021) 214.
[61] S. Sui, W. Wilson, F. Georget, H. Maraghechi, H. Kazemi-Kamyab, W. Sun, K. Scrivener, Quantification methods for chloride binding in Portland cement and limestone systems, Cem. Concr. Res. 125 (2019), 105864.
[62] Z. Shi, M.R. Geiker, K. De Weerdt, T. Østnor, B. Lothenbach, F. Winnefeld, J. Skibsted, Role of calcium on chloride binding of hydrated Portland cement – metakaolin limestone blends, Cem. Concr. Res. 95 (2017) 205–216.
[63] E. Bernard, Y. Yan, B. Lothenbach, Effective cation exchange capacity of calcium silicate hydrates (CSH), Cem. Concr. Res. 143 (2021), 106393.
[64] S.-Y. Hong, F. Glasser, Alkali binding in cement pastes: part I, The CSH phase. Cem. Concr. Res. 29 (1999) 1893–1903.
[65] H. Stade, On the reaction of CSH (di, poly) with alkali hydroxides, Cem. Concr. Res. 19 (1989) 802–810.
[66] Y. Yan, S.-Y. Yang, G.D. Miron, I.E. Collings, E. L'Hôpital, J. Skibsted, F. Winnefeld, K. Scrivener, B. Lothenbach, Effect of alkali hydroxide on calcium silicate hydrate (CSH), Cem. Concr. Res. 151 (2022), 106636.
[67] E. L'Hôpital, B. Lothenbach, K. Scrivener, D. Kulik, Alkali uptake in calcium alumina silicate hydrate (CASH), Cement and Concrete Research 85 (2016) 122–136.
[68] A. Machner, M. Bjørndal, A. Šajna, N. Mikanovic, K. De Weerdt, Impact of leaching on chloride ingress profiles in concrete, Mater. Struct. 55 (2021) 8.
[69] B. Lothenbach, F. Winnefeld, A. Leemann, LCS - Postmortem Analysis of Cement Shell, Nagra Arbeitsbericht NAB 16-034, 2016.
[70] J. Rüedi, U. Mäder, K. Kontar, A.N. Leemann, S.H. Sasamoto, C. Walker, J. Soler, LCS overcoring and analysis of borehole LGS 06-001, in: Nagra Arbeitsbericht NAB 16-025, 2012.
[71] M.J. Turrero, V. Cloet, Concrete ageing, concrete/bentonite and concrete/rock interaction analysis, in: Nagra Arbeitsbericht NAB 16-018, 2017.
[72] I. Techer, D. Bartier, P. Boulvais, E. Tinseau, K. Suchorski, J. Cabrera, A. Dauzères, Tracing interactions between natural argillites and hyper-alkaline fluids from engineered cement paste and concrete: chemical and isotopic monitoring of a 15-years old deep-disposal analogue, Appl. Geochem. 27 (2012) 1384–1402.
[73] D. Bartier, I. Techer, A. Dauzères, P. Boulvais, M.-M. Blanc-Valleron, J. Cabrera, In situ investigations and reactive transport modelling of cement paste/argillite interactions in a saturated context and outside an excavated disturbed zone, Appl. Geochem. 31 (2013) 94–108.
[74] E. Bernard, A. Jenni, M. Fisch, D. Grolimund, U. Mäder, Micro-X-ray diffraction and chemical mapping of aged interfaces between cement pastes and opalinus clay, Appl. Geochem. 115 (2020), 104538.
[75] U. Mäder, A. Jenni, C. Lerouge, S. Gaboreau, S. Miyoshi, Y. Kimura, V. Cloet, M. Fukaya, F. Claret, T. Otake, M. Shibata, B. Lothenbach, 5-year chemico-physical evolution of concrete-claystone interfaces, Swiss J. Geosci. 110 (2017) 307–327.
[76] A. Dauzères, G. Achiedo, D. Nied, E. Bernard, S. Alahrache, B. Lothenbach, Magnesium perturbation in low-pH concretes placed in clayey environment - solid characterizations and modeling, Cem. Concr. Res. 79 (2016) 137–150.
[77] C. Lerouge, S. Gaboreau, S. Grangeon, F. Claret, F. Warmont, A. Jenni, V. Cloet, U. Mäder, In situ interactions between opalinus clay and low alkali concrete, Phys. Chem. Earth, Parts A/B/C 99 (2017) 3–21.
[78] S. Gaboreau, C. Lerouge, S. Dewonck, Y. Linard, X. Bourbon, C. Fialips, A. Mazurier, D. Prêt, D. Borschneck, V. Montouillout, In-situ interaction of cement paste and shotcrete with claystones in a deep disposal context, Am. J. Sci. 312 (2012) 314–356.
[79] S. Gaboreau, D. Prêt, E. Tinseau, F. Claret, D. Pellegrini, D. Stammose, 15 years of in situ cement–argillite interaction from Tournemire URL: characterisation of the multi-scale spatial heterogeneities of pore space evolution, Appl. Geochem. 26 (2011) 2159–2171.
[80] S. Yokoyama, M. Shimbashi, D. Minato, Y. Watanabe, A. Jenni, U. Mäder, Alteration of bentonite reacted with cementitious materials for 5 and 10 years in the Mont Terri rock laboratory (CI experiment), Minerals 11 (2021) 251.
[81] M.C. Alonso, J.L.G. Calvo, J. Cuevas, M.J. Turrero, R. Fernández, E. Torres, A. I. Ruiz, Interaction processes at the concrete-bentonite interface after 13 years of FEBEX-Plug operation. Part I: Concrete alteration, Phys. Chem. Earth, Parts A/B/C 99 (2017) 38–48.
[82] B. Lothenbach, Hydration experiments of OPC, LAC and ESDRED cements: 1 h to 9 years, in: Mont Terri Technical Note TN 2016-74, Mont Terri Project, 2016.
[83] J. Olmeda, P. Henocq, E. Giffaut, M. Grivé, Modelling of chemical degradation of blended cement-based materials by leaching cycles with callovo-oxfordian porewater, Phys. Chem. Earth, Parts A/B/C 99 (2017) 110–120.
[84] A. Dauzères, P. Le Bescop, C. Cau-Dit-Coumes, F. Brunet, X. Bourbon, J. Timonen, M. Voutilainen, L. Chomat, P. Sardini, On the physico-chemical evolution of low-pH and CEM I cement pastes interacting with Callovo-Oxfordian pore water under its in situ CO2 partial pressure, Cem. Concr. Res. 58 (2014) 76–88.
[85] P. Lalan, A. Dauzères, L. De Windt, D. Bartier, J. Sammaljärvi, J.-D. Barnichon, I. Techer, V. Detilleux, Impact of a 70° C temperature on an ordinary Portland cement paste/claystone interface: an in situ experiment, Cem. Concr. Res. 83 (2016) 164–178.
[86] B. Lothenbach, E. Bernard, U. Mäder, Zeolite formation in the presence of cement hydrates and albite, Phys.Chem. Earth, Parts A/B/C 99 (2017) 77–94.
[87] R. Fernández, A.I. Ruiz, J. Cuevas, Formation of CASH phases from the interaction between concrete or cement and bentonite, Clay Miner. 51 (2016) 223–235.
[88] L. De Windt, F. Marsal, E. Tinseau, D. Pellegrini, Reactive transport modeling of geochemical interactions at a concrete/argillite interface, tournemire site (France), Phys. Chem. Earth, Parts A/B/C 33 (2008) S295–S305.
[89] N.C. Marty, C. Tournassat, A. Burnol, E. Giffaut, E.C. Gaucher, Influence of reaction kinetics and mesh refinement on the numerical modelling of concrete/clay interactions, J. Hydrol. 364 (2009) 58–72.
[90] G. Kosakowski, U. Berner, The evolution of clay rock/cement interfaces in a cementitious repository for low-and intermediate level radioactive waste, Phys. Chem. Earth, Parts A/B/C 64 (2013) 65–86.
[91] R. Fernández, D. González-Santamaría, M. Angulo, E. Torres, A.I. Ruiz, M. J. Turrero, J. Cuevas, Geochemical conditions for the formation of mg silicates phases in bentonite and implications for radioactive waste disposal, Appl. Geochem. 93 (2018) 1–9.
[92] J. Cuevas, R.V. De La Villa, S. Ramírez, L. Sánchez, R. Fernández, S. Leguey, The alkaline reaction of FEBEX bentonite: a contribution to the study of the performance of bentonite/concrete engineered barrier systems, J. Iber. Geol. 32 (2006) 151–174.
[93] R. Fernández, J. Cuevas, L. Sánchez, R.V. de la Villa, S. Leguey, Reactivity of the cement–bentonite interface with alkaline solutions using transport cells, Appl. Geochem. 21 (2006) 977–992.

[94] E. Bernard, B. Lothenbach, C. Chlique, M. Wyrzykowski, A. Dauzères, I. Pochard, C. Cau-Dit-Coumes, Characterization of magnesium silicate hydrate (M-S-H), Cement and Concrete Research 116 (2019) 309–330.
[95] M. Balonis, B. Lothenbach, G. Le Saout, F.P. Glasser, Impact of chloride on the mineralogy of hydrated Portland cement systems, Cem. Concr. Res. 40 (2010) 1009–1022.
[96] J. Haas, A. Nonat, From C-S–H to C–A–S–H: experimental study and thermodynamic modelling, Cem. Concr. Res. 68 (2015) 124–138.
[97] C. Labbez, A. Nonat, I. Pochard, B. Jönsson, Experimental and theoretical evidence of overcharging of calcium silicate hydrate, J. Colloid Interface Sci. 309 (2007) 303–307.
[98] R. Barbarulo, Comportement des matériaux cimentaires: actions des sulfates et de la température, Université Laval Québec, 2002.
[99] M. Kobayashi, K. Takahashi, Y. Kawabata, Physicochemical prperties of the Portland cement-based mortar exposed to deep seafloor conditions at a depth of 1680 m, Cem. Concr. Res. 142 (2021), 106335.
[100] R. Duval, H. Hornain, Chapitre 9: La durabilité du béton vis-à-vis des eaux aggresives, in: J. Baron, J.-P. Olivier (Eds.), La durabilité Des bétons, Presses de l'école natinoale des ponts et chaussées, Paris, France, 1992, pp. 351–391.
[101] J. Marchand, E. Samson, D. Burke, P. Tourney, N. Thaulow, S. Sahu, Predicting the Microstructural Degradation of Concrete in Marine Environment 212, ACI Symposium Publication, 2003.
[102] A. Chabrelie, E. Galluci, K. Scrivener, U. Müller, Durability of field concretes made of portland and silica fume cements under sea water exposure for 25 years, in: D.H. Bager (Ed.), Nordic Miniseminar on Nordic Exposure Sites - Input to Revision of EN206-1, Nordic Concrete Association, Hirtshals, Denmark, 2008, pp. 275–293.
[103] N.R. Buenfeld, J.B. Newman, The development and stability of surface-layers on concrete exposed to sea-water, Cem. Concr. Res. 16 (1986) 721–732.
[104] T. Danner, H.U. Jakobsen, M.R. Geiker, Mineralogical sequence of self-healing products in cracked marine concrete, Minerals 9 (2019).
[105] K. De Weerdt, H. Justnes, The effect of sea water on the phase assemblage of hydrated cement paste, Cem. Concr. Compos. 55 (2015) 215–222.
[106] E. Bernard, B. Lothenbach, C. Cau-Dit-Coumes, I. Pochard, D. Rentsch, Aluminum incorporation into magnesium silicate hydrate (M-S-H), Cem. Concr. Res. 128 (2020), 105931.
[107] E. Bernard, B. Lothenbach, C. Cau-Dit-Coumes, C. Chlique, A. Dauzères, I. Pochard, Magnesium and calcium silicate hydrates, part I: investigation of the possible magnesium incorporation in calcium silicate hydrate (C-S-H) and of the calcium in magnesium silicate hydrate (M-S-H), Applied Geochemistry 89 (2018) 229–242.
[108] T. Schmidt, B. Lothenbach, M. Romer, K.L. Scrivener, D. Rentsch, R. Figi, A thermodynamic and experimental study of the conditions of thaumasite formation, Cem. Concr. Res. 38 (2008) 337–349.
[109] N.J. Crammond, The thaumasite form of sulfate attack in the UK, Cem. Concr. Compos. 25 (2003) 809–818.
[110] M.M. Rahman, M.T. Bassuoni, Thaumasite sulfate attack on concrete: mechanisms, influential factors and mitigation, Constr. Build. Mater. 73 (2014) 652–662.
[111] A. Leemann, R. Loser, Analysis of concrete in a vertical ventilation shaft exposed to sulfate-containing groundwater for 45 years, Cem. Concr. Compos. 33 (2011) 74–83.
[112] P. Hagelia, R. Sibbick, N. Crammond, C. Larsen, Thaumasite and secondary calcite in some norwegian concretes, Cem. Concr. Compos. 25 (2003) 1131–1140.
[113] N. Crammond, R. Sibbick, G. Collett, in: Thaumasite Field Trial at Shipston on Stour: Three Year Chemical and Mineralogical Assessment of Buried Concrete 234, Special Publication, 2006, pp. 539–560.
[114] I. Sims, S.A. Huntley, The thaumasite form of sulfate attack-breaking the rules, Cem. Concr. Compos. 26 (2004) 837–844.
[115] J. Figg, Field Studies of Sulphate Attack on Concrete, The American Ceramic Society, 1999.
[116] J. Marchand, I. Odler, J.P. Skalny, Sulfate attack on concrete, CRC Press, 2001.
[117] R. Gollop, H. Taylor, Microstructural and microanalytical studies of sulfate attack. I. Ordinary portland cement paste, Cem. Concr. Res. 22 (1992) 1027–1038.
[118] X. Brunetaud, M.-R. Khelifa, M. Al-Mukhtar, Size effect of concrete samples on the kinetics of external sulfate attack, Cem. Concr. Compos. 34 (2012) 370–376.
[119] F. Bellmann, B. Möser, J. Stark, Influence of sulfate solution concentration on the formation of gypsum in sulfate resistance test specimen, Cem. Concr. Res. 36 (2006) 358–363.
[120] G. Li, P.Le Bescop, M. Moranville-Regourd, Synthesis of the U phase (4CaO· 0.9Al2O3· 1.1SO3· 0.5Na2O· 16H2O), Cement and Concrete Research 27 (1997) 7–13.
[121] D. Urushihara, T. Asaka, M. Harada, S. Kondo, M. Nakayama, M. Ogino, E. Owaki, K. Fukuda, Synthesis and structural characterization of U-phase,[3Ca2Al (OH) 6] [Na (H2O) 6 (SO4) 2· 6H2O] layered double hydroxide, J. Solid State Chem. 306 (2022), 122730.
[122] M. Santhanam, M.D. Cohen, J. Olek, Mechanism of sulfate attack: a fresh look: part 1: summary of experimental results, Cem. Concr. Res. 32 (2002) 915–921.
[123] E. Bernard, B. Lothenbach, D. Rentsch, Influence of sodium nitrate on the phases formed in the MgO-Al2O3-SiO2-H2O system, Mater. Des. 198 (2021), 109391.
[124] W. Kunther, B. Lothenbach, Improved volume stability of mortar bars exposed to magnesium sulfate in the presence of bicarbonate ions, Cem. Concr. Res. 109 (2018) 217–229.
[125] W. Kunther, B. Lothenbach, K. Scrivener, Influence of bicarbonate ions on the deterioration of mortar bars in sulfate solutions, Cem. Concr. Res. 44 (2013) 77–86.
[126] G. Zhao, J. Li, W. Shao, Effect of mixed chlorides on the degradation and sulfate diffusion of cast-in-situ concrete due to sulfate attack, Constr. Build. Mater. 181 (2018) 49–58.
[127] J. Du, Z. Tang, G. Li, H. Yang, L. Li, Key inhibitory mechanism of external chloride ions on concrete sulfate attack, Constr. Build. Mater. 225 (2019) 611–619.
[128] A. Machner, M.H. Bjørndal, H. Justnes, L. Hanžič, A. Šajna, Y. Gu, B. Bary, M. Ben Haha, M.R. Geiker, K. De Weerdt, Effect of leaching on the composition of hydration phases during chloride exposure of mortar, Cem. Concr. Res. 153 (2022), 106691.